

Causal Inference on Distribution Functions

Zhenhua Lin¹, Dehan Kong², and Linbo Wang²

¹ National University of Singapore, Singapore

² University of Toronto, Toronto, Ontario, Canada

Abstract

Understanding causal relationships is one of the most important goals of modern science. So far, the causal inference literature has focused almost exclusively on outcomes coming from the Euclidean space \mathbb{R}^p . However, it is increasingly common that complex datasets are best summarized as data points in non-linear spaces. In this paper, we present a novel framework of causal effects for outcomes from the Wasserstein space of cumulative distribution functions, which in contrast to the Euclidean space, is non-linear. We develop doubly robust estimators and associated asymptotic theory for these causal effects. As an illustration, we use our framework to quantify the causal effect of marriage on physical activity patterns using wearable device data collected through the National Health and Nutrition Examination Survey.

Keywords: Double robustness; Wasserstein space; Wearable device.

1 Introduction

Causal inference has received increasing attention in contemporary data analysis. So far, researchers in causal inference have engaged almost exclusively in studying causal effects on objects from a linear space, most commonly the Euclidean space \mathbb{R}^p . On the other hand, in many modern applications, the observed data either naturally emerge or may be summarized as distribution functions. Often in these applications, the interest lies in the causal effect on the distributions themselves, rather than a summary measure such as the mean or the quantiles. Here we detail an example from the study of physical activities; see the Supplementary Material for additional examples on cellular differentiation and metagenomics.

Example 1 (Physical Activities). *Behavioral scientists are often interested in evaluating the effects of potential risk factors, such as marriage, on physical activity patterns (e.g. King et al., 1998). The physical activity patterns are often recorded over a certain monitoring period. For example, in the National Health and Nutrition Examination Survey 2005–2006, physical activity intensity, ranging from 0 to 32767 counts per minute, was recorded consecutively for 7 days by a wearable device for subjects at least six years old. The trajectory of activity intensity is not directly comparable across different subjects as different individuals might have different circadian rhythms. Instead, the distribution of activity intensity is invariant to circadian rhythms and hence can be compared between groups of individuals (Chang and McKeague, 2020).*

On the surface, since the distribution functions belong to L^2 , a linear space endowed with a Euclidean distance, one may directly extend the classical potential outcome framework (Neyman, 1923; Rubin, 1974) in causal inference using Euclidean averages. For example, the mean potential distribution functions may be defined as the expectation of the random potential distribution function, and the causal contrast among different interventions may be defined as the Euclidean distance among the mean potential distribution functions. However, there has been a growing recognition among the statistics and data science community that in many applications, the structure of data summarized by distribution functions may be best captured by the use of non-Euclidean distances (e.g. del Barrio et al., 1999; Courty et al., 2016; Arjovsky et al., 2017; Ho et al., 2017; Bernton et al., 2019; Verdinelli et al., 2019; Panaretos and Zemel, 2019). One of the most common choices of distance is the so-called Wasserstein distance based on the geometry of optimal transport. When equipped with such a distance, the space of probabilities measures on a real interval \mathcal{I} is referred to as the Wasserstein space, and the average of distribution functions under the Wasserstein distance is known as the Wasserstein barycentre of these distributions.

Significant advances have been made by the emerging field of statistical optimal transport

studying the Wasserstein space. For instance, Agueh and Carlier (2011); Bigot et al. (2012); Kim and Pass (2017) introduced the notion of Wasserstein barycentre of a random distribution and studied its existence, uniqueness and characteristics. The concept of Wasserstein barycentre, defined in (6), is a generalization of the mean of random variables/vectors to random distributions. Moreover, Bigot et al. (2017) generalized the technique of principal component analysis to data sampled from a Wasserstein space, while Petersen and Müller (2016); Chen et al. (2021) focused on regression models for such data. Recently, Zhang et al. (2020); Zhu and Müller (2021) investigated distribution-valued time series and generalized the concept of autoregressive models to Wasserstein spaces, while Zhou et al. (2021) developed a framework for canonical correlation analysis of random distributions. For more related works on statistical data analysis in a Wasserstein space, we refer readers to the survey paper by Bigot (2020) and references therein.

The Wasserstein barycentre and distance have several features that make them particularly appealing for defining causal effects on distribution functions. First, the Wasserstein barycentre reduces to the usual Euclidean mean in the degenerate case where the distribution functions take point mass at real values. Specifically, if δ_t denotes the Dirac delta function with point mass at t , then the Wasserstein barycentre of $\delta_{t_i}, i = 1, \dots, n$ is $\delta_{\bar{t}}$, with $\bar{t} = \sum_{i=1}^n t_i/n$. In contrast, the Euclidean average, defined as the average of the cumulative distribution functions of $\delta_{t_1}, \dots, \delta_{t_n}$, corresponds to a uniform distribution on t_i, \dots, t_n . Consequently, in the degenerate case where the random distribution function takes point mass at a random real value, their expectation does not correspond to the point mass function at the expectation of the random real value.

Second, compared to the Euclidean distance and other distances such as the Hellinger distance, the Wasserstein barycentre performs exceptionally well in capturing the structure of random distributions (e.g. Cuturi and Doucet, 2014). In Figure 1, we provide a graphical illustration. The distributions in Figure 1(a) are unimodal distributions; typical distributions of this kind are adult age-at-death distributions (Chen et al., 2021). One can see from Figure 1(b) and (c) that the Wasserstein barycentre preserves unimodality while the Euclidean average does not.

Third, the Wasserstein distance has an intuitive interpretation of the amount of “work” required to transform one distribution to another (Sommerfeld and Munk, 2018). Moreover, it comes with a map that shows how to move from one random object to another, and allows one to create a path of distributions that interpolates between Wasserstein barycentres, while preserving the structural information in the random objects. This is particularly useful when comparing two Wasserstein barycentres each representing potential distribution functions under a particular intervention, as it not only contains information on how much they differ, but also

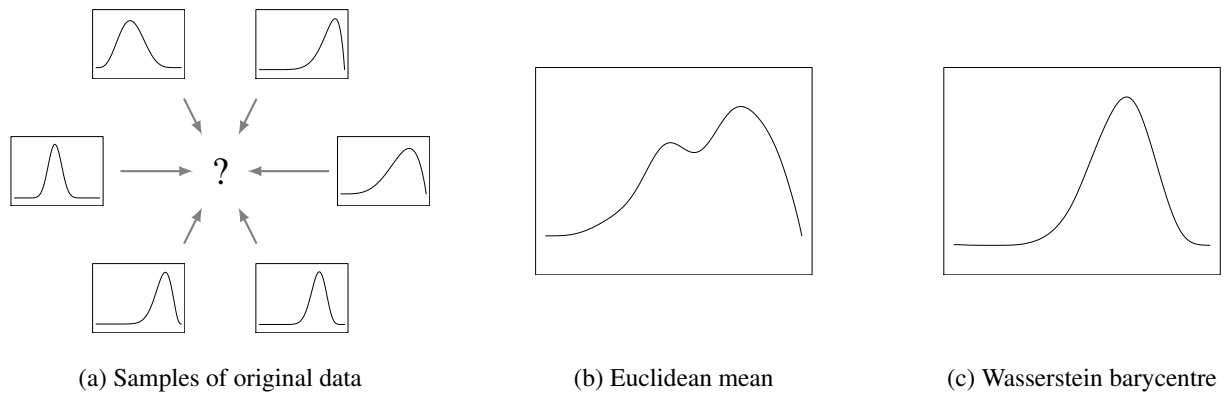


Figure 1: Comparison of Wasserstein barycentre versus Euclidean average for capturing structural information in random distributions. The barycentre and Euclidean average are based on six unimodal distributions. The Euclidean average has two modes while the Wasserstein barycentre preserves unimodality.

on how one of these barycentres can be moved to the other; see Interpretation 2 in Section 3 for more details. In fact, as the path implied by the Wasserstein distance to move distributions involves the “least effort,” it is the natural path taken by biological systems to move from one state to another (e.g. Schiebinger et al., 2019).

Lastly, in the Wasserstein space of distributions on an interval of the real line, which is the focus of this paper, the optimal way to transfer one distribution to another is to move between their corresponding quantiles. In this case, the causal effect map defined using optimal transport (see Definition 1) can be directly interpreted as the difference in quantiles of the Wasserstein barycentres of different potential outcome distributions; see Interpretation 1 in Section 3 for more details.

For these advantages and motivated by the applications in Example 1 and Examples 2, 3 in the Supplementary Material, we propose to define causal effects for distribution functions using the optimal transport between the Wasserstein barycentres of different potential outcome distributions. Our definitions of causal effect, called the average causal effect map, can be identified under straightforward generalizations of standard assumptions in the causal inference literature. We develop doubly robust and cross-fitting procedures for estimating the average causal effect map, and establish asymptotic properties for these estimators. In contrast to the setting for the classical doubly robust estimators (Robins et al., 1994; Chernozhukov et al., 2018), typically even for a fixed unit, the outcome may not be fully observed and needs to be estimated from data. For instance, in our real data application, the data consists of empirical distribution functions of physical activity patterns for individuals rather than their underlying

distribution functions. To establish the asymptotic properties with distribution-valued outcomes, our analyses rely on several geometric properties of the Wasserstein space, most notably the isometry between the Wasserstein space and the space of quantile functions. To the best of our knowledge, this is the first systematic study on causal inference for distribution-valued outcomes.

The rest of the paper is structured as follows. In Section 2, we present background on causal inference and Wasserstein space. In Section 3 we introduce the notion of average causal effect map for outcomes from a Wasserstein space, and develop identifiability results and doubly robust estimators for the average causal effect map. We then study their asymptotic properties in Section 4. We provide numerical studies in Section 5 and a real data illustration in Section 6. We end with a brief discussion in Section 7.

2 Background

2.1 The potential outcomes framework

We shall define causal effects using the potential outcomes framework. Suppose that the treatment is $A \in \{0, 1\}$, with 0 and 1 being the labels for control and active treatments, respectively. We use X to denote baseline covariates taking values in \mathbb{R}^d . For each level of treatment a , we assume there exists a potential outcome $Y(a)$, representing the outcome had the subject, possibly contrary to the fact, been given treatment a . Here $Y(a)$ is a random object that resides in a possibly non-linear space. We make the stable unit treatment value assumption (SUTVA, Rubin, 1980) so that the potential outcomes for any unit do not vary with the treatments assigned to other units, and, for each unit, there are no different versions of treatments that lead to different potential outcomes. Under this assumption, the observed outcome $Y = Y(A)$, where $Y(A) = Y(1)$ if $A = 1$ and $Y(A) = Y(0)$ if $A = 0$. We assume we observe n independent samples from an infinite super-population of (A, X, Y) , denoted by $(A_i, X_i, Y_i), i = 1, \dots, n$.

When $Y(a)$ resides in \mathbb{R} , the causal effect is commonly defined as the contrast between a summary measure of the potential outcome distributions. For example, the average causal effect is defined as the difference between the means of the potential outcome distributions:

$$\text{ACE} = \mathbb{E}\{Y(1)\} - \mathbb{E}\{Y(0)\}; \tag{1}$$

the quantile treatment effect is defined as the difference between the quantiles of the potential

outcome distributions

$$\text{QTE}(\alpha) = F_{Y(1)}^{-1}(\alpha) - F_{Y(0)}^{-1}(\alpha), \alpha \in [0, 1], \quad (2)$$

where $F_Z(z) = P(Z \leq z)$ is the cumulative distribution function (CDF) of the random variable Z and

$$F_Z^{-1}(\alpha) = \inf\{z : F_Z(z) \geq \alpha\} \quad (3)$$

is the corresponding quantile function. Causal effects defined in this manner can be interpreted on the population level, as they concern contrasts between potential outcomes in two hypothetical populations. These population-level interpretations concern the effect of introducing a particular treatment to a population and are most relevant to policy makers.

There is, however, a subtle but important distinction between the individual-level interpretations of ACE and $\text{QTE}(\alpha)$. Let $CE_i = Y_i(1) - Y_i(0)$ be the individual causal effect for unit i . Individual causal effects provide useful information for individualized treatment decision-making and are most relevant to individual subjects. Since $\text{ACE} = \mathbb{E}(CE_i)$, it can be interpreted as averages of individual causal effects; here the expectation is taken over units in the super-population. The individual-level interpretation of ACE extends to the conditional average treatment effect, $\text{CACE}(L) = \mathbb{E}\{Y(1) | L\} - \mathbb{E}\{Y(0) | L\}$, where L is a subset of observed baseline covariates. In contrast, generally, $\text{QTE}(\alpha)$ cannot be interpreted as the α -quantile of individual causal effects. This distinction connects to desideratum (d) in Section 3.1.

2.2 Causal effect identification and estimation

The following assumptions are standard in the causal inference literature (e.g. Rosenbaum and Rubin, 1983; Hernán and Robins, 2020).

Assumption 1 (Ignorability). $A \perp\!\!\!\perp Y(a) | X, a = 0, 1$.

Assumption 2 (Positivity). *The propensity score $\pi(X) := P(A = 1 | X)$ is bounded away from 0: There exists $\epsilon > 0$, such that $\epsilon < \pi(X) < 1 - \epsilon, a.e.$*

Under Assumptions 1 and 2, when $Y(a)$ resides in \mathbb{R} , the mean potential outcome is given by

$$\mu_a := \mathbb{E}[Y(a)] = \mathbb{E}_X\{\mathbb{E}[Y | A = a, X]\} = \mathbb{E}\left\{\frac{I(A = a)Y}{P(A = a | X)}\right\}. \quad (4)$$

Similarly, the potential outcome distributions $F_{Y(a)}(y)$ can be identified by replacing Y in the last term of eqn. (4) with $I(Y \leq y)$. Based on (4), the average causal effect can be identified as

ACE = $\mathbb{E}\{Y(1)\} - \mathbb{E}\{Y(0)\}$, and the quantile treatment effect can be identified as $\text{QTE}(\alpha) = F_{Y(1)}^{-1}(\alpha) - F_{Y(0)}^{-1}(\alpha)$.

Given the identification formula (4), one may use plug-in estimators to estimate the mean potential outcomes. Let $m_a(X) = \mathbb{E}(Y | A = a, X)$ and $f(A|X) = A\pi(X) + (1 - A)(1 - \pi(X))$. Also denote $\widehat{m}_a(X), \widehat{\pi}(X), \widehat{f}(A|X)$ as estimates of their corresponding population quantities obtained using standard parametric or nonparametric/machine-learning techniques. Some leading estimators of μ_a include the outcome regression estimator $\widehat{\mu}_a^{OR} = \mathbb{P}_n \widehat{m}_a(X)$, the inverse probability weighting estimator $\widehat{\mu}_a^{IPW} = \mathbb{P}_n \frac{I(A=a)Y}{\widehat{f}(A|X)}$, and the so-called doubly robust estimator $\widehat{\mu}_a^{DR} = \widehat{\mu}_a^{OR} + \mathbb{P}_n \left[\frac{I(A=a)}{\widehat{f}(A|X)} \{Y - \widehat{m}_a(X)\} \right]$; here \mathbb{P}_n refers to the empirical average operator: $\mathbb{P}_n(O) = \frac{1}{n} \sum_{i=1}^n O_i$.

2.3 Wasserstein space

Let \mathcal{I} be an interval of \mathbb{R} , V_1 and V_2 be random variables taking values in \mathcal{I} with finite second moments, and λ_1, λ_2 be their (cumulative) distribution functions, respectively. To define the Wasserstein distance between λ_1 and λ_2 , we let $\Lambda(\lambda_1, \lambda_2)$ denote all joint distributions λ_{12} of (V_1, V_2) that have marginal distributions λ_1 and λ_2 . The (2-)Wasserstein distance between λ_1 and λ_2 is defined as

$$W_2(\lambda_1, \lambda_2) = \left(\inf_{\lambda_{12} \in \Lambda(\lambda_1, \lambda_2)} \int_{\mathcal{I} \times \mathcal{I}} (s - t)^2 d\lambda_{12}(s, t) \right)^{1/2}. \quad (5)$$

The Wasserstein space of order 2 on \mathcal{I} is then defined as the space of distribution functions on \mathcal{I} with finite second moments

$$\mathcal{W}_2(\mathcal{I}) = \left\{ \lambda \text{ is a distribution function on } \mathcal{I} : \int_{\mathcal{I}} t^2 d\lambda(t) < \infty \right\}$$

endowed with the 2-Wasserstein distance.

The Wasserstein distance can be motivated by the problem of optimal transport. Consider a pile of mass on space \mathcal{I} with a distribution λ_1 . We wish to transport the mass in such a way that the new mass distribution is λ_2 . Assume also that the cost of transporting a unit mass from point s to point t is $(s - t)^2$. A transport plan to move λ_1 to λ_2 can be described by the function λ_{12} such that $d\lambda_{12}(s, t)$ denotes the amount of mass to move from s to t . Since the amount of mass to be moved out of s must match $d\lambda_1(s)$, and the amount of mass to be moved into t must match $d\lambda_2(t)$, we have $\int_{t \in \mathcal{I}} d\lambda_{12}(s, t) = d\lambda_1(s)$, $\int_{s \in \mathcal{I}} d\lambda_{12}(s, t) = d\lambda_2(t)$. In other words, $\lambda_{12} \in \Lambda(\lambda_1, \lambda_2)$. The Wasserstein distance then corresponds to the minimum effort

that is required in order to transport the mass of λ_1 to produce the mass distribution of λ_2 . The minimizer λ_{12}^* to the problem in (5) always exists (Santambrogio, 2015, Theorems 1.7 and 1.22) and is known as the optimal transport plan.

If λ_1 is continuous, then there exists a unique function $T(\cdot) : \mathcal{I} \rightarrow \mathcal{I}$ such that $d\lambda_{12}^*(s, T(s)) = d\lambda_1(s)$ (Santambrogio, 2015, Theorems 1.7 & 1.22). Intuitively, in this case, the optimal transport plan moves all the mass at s to $T(s)$. The function $T(\cdot)$ is known as the optimal transport map. Let λ^{-1} be the quantile function of the distribution λ . It can be shown that (Ambrosio et al., 2005, Theorem 6.0.2) the optimal transport map $T(s) = \lambda_2^{-1}(\lambda_1(s))$, so that it moves mass between corresponding quantiles of λ_1 and λ_2 . The following proposition, summarizing the above discussion, shows that given a fixed continuous distribution λ_1 , the distribution λ_2 can be defined via the optimal transport map from λ_1 to λ_2 . The proof of Proposition 1 is straightforward and hence omitted.

Proposition 1. *Given a continuous distribution function λ_1 , there is a one-to-one correspondence between a distribution function λ_2 and the optimal transport map from λ_1 to λ_2 .*

Based on the notion of Wasserstein distance W_2 , we can define the mean of a set of distributions $\lambda_1, \dots, \lambda_n$ in the Wasserstein space by the so-called Wasserstein barycentre $\bar{\lambda}$, defined as the distribution λ that minimizes $\frac{1}{n} \sum_{i=1}^n W_2^2(\lambda_i, \lambda)$. In Lemma 2 in the Supplementary Material, it is shown that $\bar{\lambda}^{-1} = \frac{1}{n} \sum_{i=1}^n \lambda_i^{-1}$, so that the quantile function corresponding to the Wasserstein barycentre equals the (Euclidean) averages of the individual quantile functions. The mean of distributions can also be defined in various other ways, such as the mean under the Euclidean distance $\frac{1}{n} \sum_{i=1}^n \lambda_i$. Compared to alternative center measures, the Wasserstein barycentre typically provides a better summary that captures the structure of the random objects represented by distribution functions, such as shapes, curves, and images; see for example, Figure 1 and Cuturi and Doucet (2014, Figure 1) for illustrations.

3 Causal Inference on Distribution Functions

3.1 Definition of causal effects

We now introduce a definition of average causal effect for outcomes taking value in the Wasserstein space $\mathcal{W}_2(\mathcal{I})$. In parallel to the definition of causal effects introduced in Section 2.1, we first define the mean potential outcomes. As both $Y_i(1)$ and $Y_i(0)$ take value in the Wasserstein

space, we define their means using their Wasserstein barycentres:

$$\mu_a = \mathbb{E}Y(a) \equiv \arg \min_{v \in \mathcal{W}_2(\mathcal{I})} \mathbb{E} \{W_2^2(Y(a), v)\}, \quad a = 0, 1. \quad (6)$$

Intuitively, μ_a is a “typical” potential distribution under treatment $A = a$. Let δ_t denote the Dirac delta function with point mass at t . Ideally, a causal effect definition in the Wasserstein space should satisfy the following desiderata:

- (a) When $\mathbb{E}Y(1) = \mathbb{E}Y(0)$, the causal effect equals zero;
- (b) In the degenerate case where $Y_i(a) = \delta_{y_i(a)}$, corresponding to the classical scenario where the outcome resides in \mathbb{R} , the causal effect corresponds to the usual average causal effect ACE defined in (1);
- (c) The average causal effect is a contrast between the averages of potential outcomes in two hypothetical populations, $Y(1)$ and $Y(0)$, and thus can be interpreted on the population level;
- (d) The average causal effect equals the average of individual causal effects, thus maintaining the individual-level interpretation of the ACE for real-valued outcomes discussed at the end of Section 2.1.

Desideratum (a) is natural, given the causal effect is defined as a comparison between two (hypothetical) populations. Desideratum (b) ensures that the definition is a generalization of the standard definition of the ACE (1) in the Euclidean space. Desiderata (c) and (d) are in place to ensure that the definition can be interpreted at both population and individual levels.

From an optimal transport point of view, it may be tempting to define the causal effect as the Wasserstein distance between μ_1 and μ_0 ; see Section 2 in the Supplementary Material for more discussions on causal effect defined in this way. Although causal effect defined in this way satisfies desiderata (a)–(c), in general, it fails to satisfy desideratum (d). Instead, we introduce a novel definition of average causal effect, called the *causal effect map*. In Section 3.2, we shall see that the causal effect map satisfies all the desiderata, and contains richer information than the single summary measure $W_2(\mu_1, \mu_0)$; in particular, one can compute $W_2(\mu_1, \mu_0)$ based on the causal effect map.

Definition 1. *Let λ be a continuous distribution function. The individual causal effect map of A on Y is defined as*

$$\Delta_i^\lambda(\cdot) = Y_i(1)^{-1} \circ \lambda(\cdot) - Y_i(0)^{-1} \circ \lambda(\cdot),$$

where we say λ is a reference distribution; for $a = 0, 1$, $Y_i(a)^{-1}$ is the quantile function of the distribution $Y_i(a)$ as defined in (3). The (average) causal effect map of A on Y is defined as

$$\Delta^\lambda(\cdot) = (\mathbb{E}Y(1))^{-1} \circ \lambda(\cdot) - (\mathbb{E}Y(0))^{-1} \circ \lambda(\cdot) = (\mu_1^{-1} - \mu_0^{-1}) \circ \lambda(\cdot).$$

A crucial component in Definition 1 is the choice of reference distribution λ that is allowed to have a domain different from that of Y . In general, a different reference distribution leads to a different interpretation of the causal effect maps. Hence, one should choose the reference distribution based on the desired interpretation. We now illustrate some common choices of λ with their interpretations.

Interpretation 1 (Difference in quantiles). *If the reference distribution λ is the uniform distribution on $[0, 1]$ so that $\lambda(t) = t, t \in [0, 1]$, then the causal effect map $\Delta(\cdot)$ can be interpreted as difference in quantiles.*

Remark 1. *The interpretation in terms of difference in quantiles is not to be confused with the quantile treatment effect defined in (2). In our setting, the potential outcomes are random distribution functions, and $\mu_1^{-1}(\alpha)$ is the α -quantile of the mean potential outcome under treatment. In contrast, in the quantile treatment effect setting, the realizations of potential outcomes are real numbers, and $F_{Y(1)}^{-1}(\alpha)$ is the α -quantile of the distribution of potential outcomes under treatment.*

To discuss the second interpretation, analogous to the concepts of optimal transport map, we define the *individual causal transport map* as $T_i(\cdot) = Y_i(1)^{-1} \circ Y_i(0)(\cdot)$ and the (*population*) *causal transport map* as $T(\cdot) = \mu_1^{-1} \circ \mu_0(\cdot)$. The causal transport maps are of natural interest in some applications. For example, biological experiments (Schiebinger et al., 2019) have found that cellular differentiation follows the shortest path under the Wasserstein geometry. So in Example 2, the causal transport map T describes how a group of cells would differentiate after being exposed to an intervention, measured using gene expression levels.

When the potential outcomes $Y(1), Y(0)$, and hence the barycentres μ_1 and μ_0 (e.g. Bigot et al., 2017, Proposition 4.1), are continuous distributions, with certain choices of the reference distribution, the causal effect maps can be interpreted as the (inverse of) causal transport maps up to an identity function.

Interpretation 2 (Causal transport maps). *Consider the case where the potential outcomes are random continuous distribution functions. If the reference distribution is chosen to be the barycentres μ_0 or μ_1 , then*

$$\Delta^{\mu_0} = T - \text{id} = \mu_1^{-1} \circ \mu_0 - \text{id}, \quad \Delta^{\mu_1} = \text{id} - T^{-1} = \text{id} - \mu_0^{-1} \circ \mu_1.$$

If the reference distribution is chosen to be Y_i , then

$$\Delta_i^{Y_i} = \begin{cases} T_i - \text{id} = Y_i(1)^{-1} \circ Y_i(0) - \text{id} & \text{if } A_i = 0 \\ \text{id} - T_i^{-1} = \text{id} - Y_i(0)^{-1} \circ Y_i(1) & \text{if } A_i = 1 \end{cases}. \quad (7)$$

3.2 Properties of causal effect maps

We now describe several desirable properties of the causal effect maps. First, it is easy to verify that for any choice of reference distribution λ , the causal effect map satisfies desiderata (a)–(c). The following theorem, which is crucial for identification of the average causal effect map as we shall see later in Section 3.3, shows that the causal effect map also satisfies desideratum (d). This theorem can be proved using Lemma 2 in the Supplementary Material.

Theorem 1. *The average causal effect map corresponds to the average of individual causal effect maps with respect to the same reference distribution λ :*

$$\Delta^\lambda(\cdot) = \mathbb{E}\Delta_i^\lambda(\cdot) = \mathbb{E}\{Y(1)^{-1} \circ \lambda(\cdot) - Y(0)^{-1} \circ \lambda(\cdot)\}.$$

Remark 2. *In contrast to Theorem 1, the population causal transport map is generally different from the average of individual causal transport maps: $T \neq \mathbb{E}[T_i]$. To see this, note that as shown in Interpretation 2, $T = \Delta^{\mu_0} + \text{id}$, while $T_i = \Delta_i^{Y_i(0)} + \text{id}$. Although as we show in Theorem 1, under the same reference distribution λ , $\Delta^\lambda = \mathbb{E}\Delta_i^\lambda$, in general, $\Delta^{\mu_0} \neq \mathbb{E}\Delta_i^{Y_i(0)}$. Instead, as we illustrate later in Section 6, to estimate the (expectation of) causal transport map for a particular individual i , one first estimates the average causal effect map with reference distribution Y_i , and then applies (7).*

In some scenarios, practitioners may also want a scalar quantity that measures the magnitude of the causal effect. The Wasserstein distance is a natural choice from an optimal transport point of view. The following proposition shows that one may compute the Wasserstein distance $W_2(\mu_1, \mu_0)$ from the causal effect map $\Delta^\lambda(\cdot)$. In particular, for any U that follows the reference distribution λ , $W_2(\mu_1, \mu_0)$ equals the ℓ_2 -norm of $\Delta^\lambda(U)$. It can be proved using Lemma 1 in the Supplementary Material.

Proposition 2. *The Wasserstein distance $W_2(\mu_1, \mu_0)$ is determined by the causal effect map $\Delta^\lambda(\cdot)$ via*

$$W_2(\mu_1, \mu_0) = \|\Delta^\lambda\|_\lambda := \left\{ \mathbb{E}_{U \sim \lambda} (\Delta^\lambda)^2(U) \right\}^{1/2} = \left\{ \int (\Delta^\lambda)^2(u) d\lambda(u) \right\}^{1/2}.$$

3.3 Identification and estimation

Under the ignorability and positivity assumptions, similar to (4), we can identify the causal effect map Δ^λ .

Theorem 2. *Under Assumptions 1 and 2, the average causal effect map Δ^λ is identifiable and given by*

$$\Delta^\lambda = \mu_1^{-1,\lambda} - \mu_0^{-1,\lambda}$$

with

$$\mu_a^{-1,\lambda} = \mathbb{E}_X \left\{ \mathbb{E}[(Y^{-1} \circ \lambda) | A = a, X] \right\} = \mathbb{E} \left\{ \frac{I(A = a)(Y^{-1} \circ \lambda)}{P(A = a | X)} \right\}.$$

To see the above, note that

$$\begin{aligned} \Delta^\lambda &= \sum_{a=0,1} (2a - 1) \mathbb{E} \{ Y(a)^{-1} \circ \lambda \} \quad (\text{due to Theorem 1}) \\ &= \sum_{a=0,1} (2a - 1) \mathbb{E}_X [\mathbb{E} \{ Y(a)^{-1} \circ \lambda | A = a, X \}] \quad (\text{due to ignorability}) \\ &= \sum_{a=0,1} (2a - 1) \mathbb{E}_X [\mathbb{E} \{ Y^{-1} \circ \lambda | A = a, X \}] \quad (\text{due to the SUTVA}) \\ &= \mu_1^{-1,\lambda} - \mu_0^{-1,\lambda}. \end{aligned}$$

Remark 3. *In general, when $Y(a)$ is a random distribution function,*

$$\mu_a \neq \mathbb{E}_X \{ \mathbb{E}[Y | A = a, X] \} = \mathbb{E} \left\{ \frac{I(A = a)Y}{P(A = a | X)} \right\}.$$

So $\mu_a, a = 0, 1$ may not be directly identified using the identification formula (4) for real-valued Y . Instead, following Theorem 2, the mean potential outcomes $\mu_a, a = 0, 1$ may be identified as the inverse of $\mu_a^{-1,\lambda} \circ \lambda^{-1}$.

Remark 4. *When the outcome is a distribution function, Assumption 1 is stronger than the same assumption applied to a summary measure of the outcome.*

Similar to Section 2.2, we let $m_a^\lambda(X) = \mathbb{E}\{Y^{-1} \circ \lambda | A = a, X\}$, so that $\Delta^\lambda = \sum_{a=0,1} (2a - 1) \mathbb{E}_X m_a^\lambda(X)$. We consider a regression model $m_a^\lambda(X; \beta)$, where β may be finite or infinite dimensional. In practice, the outcome Y_i , which is a distribution function itself, might not be fully observed. Instead, we typically only observe k_i samples from Y_i . We hence propose to construct a doubly robust estimator for Δ^λ in the following steps: (i) Use standard nonparametric methods such as the nonparametric maximum likelihood estimation, or local polynomial smoothing

to obtain the estimates \widehat{Y}_i ; (ii) If λ is unknown, obtain an estimate of λ , denoted as $\widehat{\lambda}$; for notational convenience, we let $\widehat{\lambda} = \lambda$ if λ is a fixed or fully observed reference distribution; (iii) Regress $\widehat{Y}^{-1} \circ \widehat{\lambda}$ on X and A to obtain an estimate of $m_a^\lambda(X)$ for each individual in the sample, denoted as $\widehat{m}_a^{\widehat{\lambda}}(X_i)$, $i = 1, \dots, n$; this may be done using a standard functional regression model (see e.g. Ramsay and Silverman, 2005, Chapter 13); (iv) Construct an estimate for $f(A|X)$, denoted as $\widehat{f}(A|X)$; (v) Construct a doubly robust estimator via

$$\widehat{\Delta}_{DR}^{\widehat{\lambda}} = \widehat{\mu}_1^{-1, \widehat{\lambda}} - \widehat{\mu}_0^{-1, \widehat{\lambda}} \quad \text{with} \quad \widehat{\mu}_a^{-1, \widehat{\lambda}} = \mathbb{P}_n \left[\widehat{m}_a^{\widehat{\lambda}}(X) + \frac{I(A=a)}{\widehat{f}(A|X)} \left\{ \widehat{Y}^{-1} \circ \widehat{\lambda} - \widehat{m}_a^{\widehat{\lambda}}(X) \right\} \right]. \quad (8)$$

This estimator, motivated by the doubly robust estimator discussed in Section 2.2, combines an outcome regression estimator with an inverse probability weighting estimator. We establish its asymptotic properties in Section 4.

In the doubly robust estimating procedure described above, the data are used twice: once for estimating $\widehat{\pi}$, \widehat{f} and $\widehat{m}_a^{\widehat{\lambda}}$, and once for estimating the causal effect $\widehat{\Delta}_{DR}^{\widehat{\lambda}}$. Theoretical analysis of such estimators is rather challenging and requires some complex conditions that may fail in settings involving machine learning methods; see Assumption 7 and Remark 5. To overcome this difficulty, following Chernozhukov et al. (2018), we propose the following cross-fitting estimators. The entire data are randomly partitioned into K parts of roughly equal sizes, denoted by $\mathcal{D}_1, \dots, \mathcal{D}_K$. For $k = 1, \dots, K$, we use $\mathcal{D}_{-k} = \cup_{m \neq k} \mathcal{D}_m$ to obtain estimates \widehat{f}_k , $\widehat{\pi}_k$, $\widehat{m}_{a,k}^{\widehat{\lambda}_k}$ and $\widehat{\lambda}_k$ (if λ is chosen to be an unknown distribution), and use \mathcal{D}_k to estimate the causal effect by $\widehat{\Delta}_{CF,k}^{\widehat{\lambda}_k} = \widehat{\mu}_{1,k}^{-1, \widehat{\lambda}_k} - \widehat{\mu}_{0,k}^{-1, \widehat{\lambda}_k}$, where

$$\widehat{\mu}_{a,k}^{-1, \widehat{\lambda}_k} = n_k^{-1} \sum_{i \in \mathcal{D}_k} \left[\widehat{m}_{a,k}^{\widehat{\lambda}_k}(X_i) + \frac{I(A_i=a)}{\widehat{f}_k(A_i|X_i)} \left\{ \widehat{Y}_i^{-1} \circ \widehat{\lambda}_k - \widehat{m}_{a,k}^{\widehat{\lambda}_k}(X_i) \right\} \right],$$

where n_k is the sample size of the k th partition. Finally, we combine the effects from different partitions via

$$\widehat{\mu}_{a,CF}^{-1, \widehat{\lambda}} = \sum_{k=1}^K \frac{n_k}{n} \widehat{\mu}_{a,k}^{-1, \widehat{\lambda}_k} \circ \widehat{\lambda}_k^{-1} \circ \widehat{\lambda} \quad \text{and} \quad \widehat{\Delta}_{CF}^{\widehat{\lambda}} = \widehat{\mu}_{1,CF}^{-1, \widehat{\lambda}} - \widehat{\mu}_{0,CF}^{-1, \widehat{\lambda}}, \quad (9)$$

where $\widehat{\lambda}$ is estimated using the entire dataset. In the above, if each reference distribution $\widehat{\lambda}_k$ is fixed to a common distribution $\widehat{\lambda}$, then (9) is reduced to $\widehat{\Delta}_{CF}^{\widehat{\lambda}} = n^{-1} \sum_{k=1}^K n_k \widehat{\Delta}_{CF,k}^{\widehat{\lambda}}$. Otherwise, the objects $\widehat{\Delta}_{CF,k}^{\widehat{\lambda}_k}$ reside in distinct spaces $L^2(\mathcal{J}; \widehat{\lambda}_k)$ for $k = 1, \dots, K$, where \mathcal{J} is the domain of λ . In this case, to combine $\widehat{\Delta}_{CF,k}^{\widehat{\lambda}_k}$, in (9) we apply the optimal transport between the measures $\widehat{\lambda}_k$ and $\widehat{\lambda}$ to move it from the space $L^2(\mathcal{J}; \widehat{\lambda}_k)$ into the space $L^2(\mathcal{J}; \widehat{\lambda})$.

To reduce the sensitivity of the cross-fitting estimator to partitioning, as suggested by Chernozhukov et al. (2018), one may repeat the estimator $\widehat{\Delta}_{CF}^{\widehat{\lambda}}$ for R times over independent partitioning. This results in estimates $\widehat{\Delta}_{CF}^{\widehat{\lambda},r}$ for $r = 1, \dots, R$. We then estimate Δ^λ by

$$\widehat{\Delta}_{CF}^{\widehat{\lambda},med}(\cdot) = \text{median}\{\widehat{\Delta}_{CF}^{\widehat{\lambda},r}(\cdot)\}_{r=1}^R. \quad (10)$$

4 Asymptotic Properties

We study the asymptotic properties of the proposed estimators, including $\widehat{\Delta}_{DR}^{\widehat{\lambda}}$ and $\widehat{\Delta}_{CF}^{\widehat{\lambda}}$, in this section. Let \mathcal{J} , potentially coincides with \mathcal{I} , be the domain of the reference distribution λ . For simplicity, we assume \mathcal{I} and \mathcal{J} to be a bounded interval of \mathbb{R} . This condition may be replaced by some moment conditions on Y_i and other relevant quantities; see Remarks 8 and 9 in the Supplementary Material for details.

In the following, we shall first introduce assumptions on the variability from estimating $Y_i, i = 1, \dots, n$ and λ .

Assumption 3. *The estimates $\widehat{Y}_1, \dots, \widehat{Y}_n$ are independent, and there are two sequences of constants $\alpha_n = o(1)$ and $\nu_n = o(1)$ such that*

$$\begin{aligned} \sup_{1 \leq i \leq n} \sup_{v \in \mathcal{W}_2(\mathcal{I})} \mathbb{E}\{W_2^2(\widehat{Y}_i, Y_i) | Y_i = v\} &= O(\alpha_n^2), \\ \sup_{1 \leq i \leq n} \sup_{v \in \mathcal{W}_2(\mathcal{I})} \text{var}\{W_2^2(\widehat{Y}_i, Y_i) | Y_i = v\} &= O(\nu_n^4). \end{aligned} \quad (11)$$

The conditional expectation $\mathbb{E}[W_2^2(\widehat{Y}_i, Y_i) | Y_i]$ in Assumption 3 is a real-valued measurable function defined on $\mathcal{W}_2(\mathcal{I})$, the precise definition of which is given in Section 3 of the Supplementary Material. Assumption 3 requires that $\widehat{Y}_i, i = 1, \dots, n$, converge to their population counterparts at certain rates. Suppose that the number of observations for unit i , $k_i \asymp n^\zeta$ for some constant $\zeta > 0$. If \widehat{Y}_i is obtained using the corresponding empirical distribution function, then under some additional moment assumptions, condition (11) holds with $\alpha_n^2 = \nu_n^4 = n^{-\zeta/2}$. This can be shown via a combination of Fournier and Guillin (2015, Theorem 1) and Santambrogio (2015, Proposition 2.17). Assumption 3 also holds with many other standard non-parametric estimators for Y_i . For example, under some regularity conditions on the distribution of Y , the estimator by Petersen and Müller (2016) satisfies condition (11) with a faster rate: $\alpha_n^2 = n^{-2\zeta/3}$ and $\nu_n^4 = n^{-4\zeta/3}$.

The following Assumption 4 imposes a condition on the rate of convergence for $\widehat{\lambda}$. It is satisfied, for example, when λ is a fixed and known distribution so that $\widehat{\lambda} = \lambda$. Under Assumption 3, it holds for $\lambda = Y_i$. It also holds when λ is the Fréchet mean of Y_i and $\widehat{\lambda} = \arg \min_{v \in \mathcal{W}_2(\mathcal{I})} \sum_{i=1}^n W_2^2(v, \widehat{Y}_i)$ is the sample Fréchet mean; see Lemma 7 in the Supplementary Material.

Assumption 4. $W_2^2(\widehat{\lambda}, \lambda) = O_P(n^{-1} + \alpha_n^2 + \nu_n^2)$.

Let \tilde{m}_a^λ be an estimate of m_a^λ by using the outcome $Y_i, i = 1, \dots, n$ and λ . To study the asymptotic properties of the causal effect map estimator $\widehat{\Delta}_{DR}^\lambda$, we introduce Assumption 5 that is standard in causal effect estimation (e.g. Hernán and Robins, 2020). Part (a) of Assumption 5 assumes positivity of the estimated propensity scores, while part (b) assumes that \tilde{m}_a^λ and $\widehat{\pi}$ converge to their limits uniformly.

Assumption 5.

- (a) *The estimated propensity scores are bounded away from zero: for some $\epsilon > 0$, $\text{pr}\{\inf_x \widehat{\pi}(x) > \epsilon \text{ and } \sup_x \widehat{\pi}(x) < 1 - \epsilon\} = 1$.*
- (b) *The outcome regression and propensity score estimates converge: $\sup_x \|\tilde{m}_a^\lambda(x) - m_a^{\lambda,*}(x)\|_\lambda = o_P(1)$, $a = 0, 1$ and $\sup_x |\widehat{\pi}(x) - \pi^*(x)| = o_P(1)$ for some functions $m_a^{\lambda,*}$ and π^* .*

The following Assumption 6 assumes that the outcome regression estimates \widehat{m}_a^λ obtained using $\widehat{\lambda}$ and $\widehat{Y}_i, i = 1, \dots, n$ are not too far away from the quantities \tilde{m}_a^λ . It holds for estimators $\widehat{m}_a^\lambda(x)$ that are Lipschitz continuous functions of a weighted average of $(\widehat{Y}_1)^{-1} \circ \lambda, \dots, (\widehat{Y}_n)^{-1} \circ \lambda$. Examples include local polynomial estimators and parametric estimators satisfying certain regularity conditions. Note that the optimal transport $\widehat{\lambda}^{-1} \circ \lambda$ in the assumption is needed to transport \widehat{m}_a^λ , which resides in the space $L^2(\mathcal{J}; \widehat{\lambda})$, into the space $L^2(\mathcal{J}; \lambda)$ where \tilde{m}_a^λ resides.

Assumption 6. $\mathbb{P}_n \|\widehat{m}_a^\lambda(X) \circ \widehat{\lambda}^{-1} \circ \lambda - \tilde{m}_a^\lambda(X)\|_\lambda^2 = O_P(W_2^2(\widehat{\lambda}, \lambda) + \alpha_n^2 + \nu_n^2)$ for $a = 0, 1$.

To state the last condition, we first define the concept of Donsker class. Consider a fixed $a \in \{0, 1\}$. For a real number $t \in \mathcal{J}$, a function $\check{m}^\lambda : \mathcal{X} \rightarrow \mathcal{L}_\lambda(\mathcal{W}_2(\mathcal{I})) := \{v^{-1} \circ \lambda : v \in \mathcal{W}_2(\mathcal{I})\}$ and a function $\check{\pi} : \mathcal{I} \rightarrow \mathbb{R}$, we view the element $t \times \check{m}^\lambda \times \check{\pi}$ as a real-valued function defined on (A, X, Y) by

$$(t \times \check{m}^\lambda \times \check{\pi})(A, X, Y) = \frac{(aA + (1-a)(1-A))\{(Y^{-1} \circ \lambda)(t) - \check{m}_a^\lambda(X)(t)\}}{a\check{\pi}(X) + (1-a)(1-\check{\pi}(X))} + \check{m}_a^\lambda(X)(t),$$

and for a family \mathcal{F}_a^λ of functions in the form of $t \times \check{m}^\lambda \times \check{\pi}$, we view $\sqrt{n}\mathcal{G}_a(t \times \check{m}^\lambda \times \check{\pi}) := \sqrt{n}(\mathbb{P}_n - \mathbb{E})\{(t \times \check{m}^\lambda \times \check{\pi})(A, X, Y)\}$ as a real-valued random process indexed by functions in

\mathcal{F}_a^λ . Let $L^\infty(\mathcal{F}_a^\lambda)$ denote the collection of real-valued functions H defined on \mathcal{F}_a^λ and satisfying $\sup_{q \in \mathcal{F}_a^\lambda} |H(q)| < \infty$. We say \mathcal{F}_a^λ is a Donsker class if $\sqrt{n}\mathbb{G}_a$ converges to a tight Gaussian measure on $L^\infty(\mathcal{F}_a^\lambda)$.

Let \mathcal{M}_a^λ be a class of functions containing m_a^λ . For $g, h \in \mathcal{M}_a^\lambda$, define $\eta_i(g, h) = \|g(X_i) - h(X_i)\|_\lambda$ and $\eta^2(g, h) = n^{-1} \sum_{i=1}^n \eta_i^2(g, h)$. Conditional on $\mathbb{X} = (X_1, \dots, X_n)$, η defines a pseudo-distance function on \mathcal{M}_a^λ . Let $B_a(r; g) = \{h \in \mathcal{M}_a^\lambda : \eta(g, h) < r\}$ be a ball in \mathcal{M}_a^λ with radius r , and $N_a(\delta, r, \eta)$ denote the smallest number of δ -balls in the pseudo-metric space $(\mathcal{M}_a^\lambda, \eta)$ that are required to cover $B_a(r; m_a)$. Without loss of generality, we assume $N_a(\delta, r, \eta)$ is continuous in δ and r . Otherwise, we just redefine it with its continuous upper bound.

The following Assumption 7 imposes some technical conditions on the estimators $\widehat{\pi}$ and \widehat{m}_a^λ . Part (a) assumes that each data point has an asymptotically equal contribution to the estimators, i.e., there is no outlier in the sense that as the sample size grows, the influence of a single data point on the estimates $\widehat{\pi}$ and \widehat{m}_a^λ is negligible. Part (b) restricts \mathcal{F}_a^λ to be a Donsker class, and part (c) limits the complexity of \mathcal{M}_a^λ via a bound on the metric entropy, which enables us to employ empirical process theory to provide an upper bound on the convergence rate of $\widehat{\Delta}_{DR}^\lambda$. These conditions are satisfied, for example, by a logistic model for π and a simple linear regression model for m_a^λ .

Assumption 7.

- (a) *Stability of the estimators: For a constant $C_4 > 0$, $\sup_{1 \leq i \leq n} \mathbb{E} |\widehat{\pi}(X_i) - \widehat{\pi}_{-i}(X_i)|^2 \leq C_4 n^{-1}$ and $\sup_a \sup_{1 \leq i \leq n} \mathbb{E} \|\widehat{m}_a^\lambda(X_i) - \widehat{m}_{a,-i}^\lambda(X_i)\|_\lambda^2 \leq C_4 n^{-1}$, where $\widehat{\pi}_{-i}$ and $\widehat{m}_{a,-i}^\lambda$ are the estimates of π and m_a^λ without using the i th subject, respectively.*
- (b) *For $a = 0, 1$, the class \mathcal{F}_a^λ is a Donsker class containing $t \times m_a^{\lambda,*} \times \pi^*$ for all t , and with probability tending to one, $t \times \widehat{m}_a^\lambda \times \widehat{\pi} \in \mathcal{F}_a^\lambda$ for all t .*
- (c) *For $a = 0, 1$, for some fixed $K > 0$, $\widehat{m}_a^\lambda \in \mathcal{M}_a^\lambda$, $\widehat{m}_a^{\widehat{\lambda}}(\cdot) \circ \widehat{\lambda}^{-1} \circ \lambda \in \mathcal{M}_a^\lambda$, and $\log N_a(\delta, r, \eta) \leq Kr\delta^{-1}$ for all $r, \delta > 0$ almost surely.*

Remark 5. Assumption 7 may fail in settings invoking machine learning methods, in which case the dimension of covariates X is modelled as an increasing function of the sample size (Chernozhukov et al., 2018). Notably Theorem 4 for the cross-fitting estimator $\widehat{\Delta}_{CF}^\lambda$ does not require this assumption and thus can accommodate machine learning methods for modeling π and m_a^λ .

Let $\|\widehat{m}_a^\lambda - m_a^\lambda\|_\lambda^2 = \int \|\widehat{m}_a^\lambda(x) - m_a^\lambda(x)\|_\lambda^2 dF_X(x)$, the integrated squared error of \widehat{m}_a^λ for estimating m_a^λ , where F_X denotes the probability measure induced by X . Similarly, the integrated

squared error of $\widehat{\pi}$ for estimating π is denoted by $\|\widehat{\pi} - \pi\|_2^2 = \int |\widehat{\pi}(x) - \pi(x)|^2 dF_X(x)$. Define $\varrho_\pi^4 := \varrho_\pi^4(n) := \mathbb{E}\|\widehat{\pi} - \pi\|_2^4$ and $\varrho_m^4 := \varrho_m^4(n) := \max\{\mathbb{E}\|\widehat{m}_0^\lambda - m_0^\lambda\|_\lambda^4, \mathbb{E}\|\widehat{m}_1^\lambda - m_1^\lambda\|_\lambda^4\}$. Let $L^2(\lambda) = \{h \in \mathbb{R}^{\mathcal{J}} : \int_{\mathcal{J}} |h|^2 d\lambda < \infty\}$ be endowed with the inner product $\langle h_1, h_2 \rangle_\lambda = \int_{\mathcal{J}} h_1 h_2 d\lambda$ and the induced norm $\|h\|_\lambda = \langle h, h \rangle_\lambda^{1/2}$. Finally, let

$$\varphi(A, X, Y) = \frac{A\{Y^{-1} \circ \lambda - m_1^\lambda(X)\}}{\pi(X)} + m_1^\lambda(X) - \frac{(1-A)\{Y^{-1} \circ \lambda - m_0^\lambda(X)\}}{1 - \pi(X)} - m_0^\lambda(X).$$

The following Theorem 3 shows that the estimator $\widehat{\Delta}_{DR}^{\widehat{\lambda}}$ enjoys the double robustness property whether $\widehat{\lambda}$ is a fixed and known distribution or is estimated from data, so that the convergence rate is $n^{-1/2}$ when either of ϱ_π and ϱ_m is of the order $n^{-1/2}$ and the other one is bounded. Moreover, one may use flexible non-parametric methods for estimating $m_a^\lambda, a = 0, 1$ and π , provided that the nonparametric convergence rates satisfy $\varrho_m \varrho_\pi = o(n^{-1/2})$. Theorem 3 also shows that $\widehat{\Delta}_{DR}^{\widehat{\lambda}}$ is an asymptotically linear estimator with influence function $\varphi(A, X, Y) - \mathbb{E}\varphi(A, X, Y)$.

Theorem 3. *Suppose that both $\widehat{\lambda}$ and λ are continuous distribution functions. If Assumptions 1–7 hold with $\alpha_n = o(n^{-1/2})$ and $\nu_n = o(n^{-1/2})$, then*

- (i) $\|\widehat{\Delta}_{DR}^\lambda \circ \widehat{\lambda}^{-1} \circ \lambda - \Delta^\lambda\|_\lambda = O_P(n^{-1/2} + n^{-1/2} \varrho_m^{1/2} + n^{-1/2} \varrho_\pi + \varrho_m \varrho_\pi)$;
- (ii) if $\varrho_m \varrho_\pi = o(n^{-1/2})$, $\varrho_m = o(1)$, $\varrho_\pi = o(1)$, then $\sqrt{n}(\widehat{\Delta}_{DR}^\lambda \circ \widehat{\lambda}^{-1} \circ \lambda - \Delta^\lambda) = \sqrt{n}(\mathbb{P}_n - \mathbb{E})\{\varphi(A, X, Y)\} + o_P(1)$, and consequently $\sqrt{n}(\widehat{\Delta}_{DR}^\lambda \circ \widehat{\lambda}^{-1} \circ \lambda - \Delta^\lambda)$ converges weakly to a centered Gaussian process in the space $L^2(\mathcal{J}; \lambda)$ with the same asymptotic distribution as $\sqrt{n}(\mathbb{P}_n - \mathbb{E})\{\varphi(A, X, Y)\}$.

Remark 6. *The covariance function of the limit distribution of $\sqrt{n}(\mathbb{P}_n - \mathbb{E})\{\varphi(A, X, Y)\}$ can be*

estimated from data, as follows. Let $V = \frac{A\{Y^{-1} \circ \lambda - m_1^\lambda(X)\}}{\pi(X)} + m_1^\lambda(X) - \frac{(1-A)\{Y^{-1} \circ \lambda - m_0^\lambda(X)\}}{1 - \pi(X)} - m_0^\lambda(X)$ and $G = \sqrt{n}(\mathbb{P}_n - \mathbb{E})\{\varphi(A, X, Y)\}$. Then G and its limit distribution share the same covariance function of V . Letting $\widehat{V}_i = \frac{A_i\{\widehat{Y}_i^{-1} \circ \widehat{\lambda} - \widehat{m}_1^\lambda(X_i)\}}{\widehat{\pi}(X_i)} + \widehat{m}_1^\lambda(X_i) - \frac{(1 - A_i)\{\widehat{Y}_i^{-1} \circ \widehat{\lambda} - \widehat{m}_0^\lambda(X_i)\}}{1 - \widehat{\pi}(X_i)} - \widehat{m}_0^\lambda(X_i)$, we can use the sample covariance $\widehat{C}(s, t) = n^{-1} \sum_{i=1}^n \{V_i(s) - \bar{V}(s)\} \{V_i(t) - \bar{V}(t)\}$ as an estimate of the covariance function of V , where $s, t \in \mathcal{J}$ and $\bar{V} = n^{-1} \sum_{i=1}^n V_i$.

Remark 7. *The above asymptotic result enables inference on Δ^λ . Take the case that λ is fixed and known so that $\widehat{\lambda} = \lambda$ for example. An approximate simultaneous confidence band (SCB) in the form of $[\widehat{\Delta}_{DR}^\lambda(t) - q_{\alpha/2} n^{-1/2}, \widehat{\Delta}_{DR}^\lambda(t) + q_{\alpha/2} n^{-1/2}]$ with a constant $q_{\alpha/2}$ for all $t \in \mathcal{J}$, i.e., $P\{\sup_{t \in \mathcal{J}} \sqrt{n} |\widehat{\Delta}_{DR}^\lambda(t) - \Delta^\lambda(t)| \leq q_{\alpha/2}\} \approx 1 - \alpha$ for a significance level α , can be derived for Δ^λ , by estimating $q_{\alpha/2}$ via a resampling strategy. Specifically, we draw B realizations G_1, \dots, G_B ,*

for example, $B = 1000$, from the centered Gaussian process with the covariance \widehat{C} , and for each realization G_j we compute $g_j = \sup_{t \in \mathcal{J}} |G_j(t)|$. Then $q_{\alpha/2}$ is estimated by the $1 - \alpha/2$ empirical quantile $\widehat{q}_{\alpha/2}$ of g_1, \dots, g_B , and the approximate SCB is given by $[\widehat{\Delta}_{DR}^\lambda(t) - \widehat{q}_{\alpha/2} n^{-1/2}, \widehat{\Delta}_{DR}^\lambda(t) + \widehat{q}_{\alpha/2} n^{-1/2}]$. With the derived SCB, one can also test the null hypothesis $\Delta^\lambda \equiv 0$, for example, by rejecting the null at the significance level α if $0 \notin [\widehat{\Delta}_{DR}^\lambda(t) - \widehat{q}_{\alpha/2} n^{-1/2}, \widehat{\Delta}_{DR}^\lambda(t) + \widehat{q}_{\alpha/2} n^{-1/2}]$ for some $t \in \mathcal{J}$. Note that the same procedure applies to the estimator $\widehat{\Delta}^{\widehat{\lambda}}$ and the cross-fitting estimators in light of the theorems in the sequel.

Next we turn to the cross-fitting estimator (9) and show that it enjoys double robustness and asymptotic normality properties without the technical assumption 7 (e.g. Chernozhukov et al., 2018). For this, we require that the sizes of the partitions are of the same order, quantified by Assumption 9, and we tailor Assumption 6 to the cross-fitting estimator by Assumption 8. Let $\tilde{m}_{a,k}^\lambda$, the counterpart of $\widehat{m}_{a,k}^{\widehat{\lambda}}$, be estimated by using the outcomes Y_i (instead of \widehat{Y}_i) and the reference distribution λ (instead of $\widehat{\lambda}$).

Assumption 8. $\left\| \widehat{m}_{a,k}^{\widehat{\lambda}_k}(\cdot) \circ \widehat{\lambda}_k^{-1} \circ \lambda - \tilde{m}_{a,k}^\lambda \right\|_\lambda^2 = O_P(W_2^2(\widehat{\lambda}_k, \lambda) + \alpha_n^2 + \nu_n^2)$ for $a = 0, 1$ and $k = 1, \dots, K$.

Assumption 9. There exist constants c_1 and c_2 such that $0 < c_1 \leq n_k/n \leq c_2 < 1$ for all n and $k = 1, \dots, K$.

Theorem 4. Suppose that both $\widehat{\lambda}$ and λ are continuous distribution functions. If Assumptions 1–3 and 8–9 hold with $\alpha_n = o(n^{-1/2})$ and $\nu_n = o(n^{-1/2})$, and additionally, Assumptions 4–5 hold for $\widehat{m}_{a,k}^{\widehat{\lambda}}$, $\tilde{m}_{a,k}^\lambda$, $\widehat{\pi}$ and $\widehat{\lambda}_k$ for $k = 1, \dots, K$, then for the estimator defined in (9), we have

$$(i) \quad \left\| \widehat{\Delta}_{CF}^{\widehat{\lambda}} \circ \widehat{\lambda}^{-1} \circ \lambda - \Delta^\lambda \right\|_\lambda = O_P(n^{-1/2} + n^{-1/2} \varrho_m + n^{-1/2} \varrho_\pi + \varrho_m \varrho_\pi);$$

(ii) if $\varrho_m \varrho_\pi = o(n^{-1/2})$, $\varrho_m = o(1)$, $\varrho_\pi = o(1)$, then $\sqrt{n} \left(\widehat{\Delta}_{CF}^{\widehat{\lambda}} \circ \widehat{\lambda}^{-1} \circ \lambda - \Delta^\lambda \right) = \sqrt{n} (\mathbb{P}_n - \mathbb{E}) \{ \varphi(A, X, Y) \} + o_P(1)$, and consequently $\sqrt{n} \left(\widehat{\Delta}_{CF}^{\widehat{\lambda}} \circ \widehat{\lambda}^{-1} \circ \lambda - \Delta^\lambda \right)$ converges weakly to a centered Gaussian process in the space $L^2(\mathcal{J}; \lambda)$ with the same asymptotic distribution as $\sqrt{n} (\mathbb{P}_n - \mathbb{E}) \{ \varphi(A, X, Y) \}$.

The above results show that the cross-fitting estimator $\widehat{\Delta}_{CF}^{\widehat{\lambda}}$ also enjoys double robustness. A simultaneous confidence band for $\widehat{\Delta}_{CF}^{\widehat{\lambda}}$ can be constructed using the method described in Remark 7. For the estimator $\widehat{\Delta}_{CF}^{\widehat{\lambda}, med}$ in (10), as in Chernozhukov et al. (2018), the covariance function $C(\cdot, \cdot)$ of the process $\sqrt{n} (\mathbb{P}_n - \mathbb{E}) \{ \varphi(A, X, Y) \}$ may be estimated as follows. For $r = 1, 2, \dots, R$, let $\widetilde{C}^r(s, t) = \widehat{C}^r(s, t) + \{ \widehat{\Delta}_{CF}^{\widehat{\lambda}, r}(s) - \widehat{\Delta}_{CF}^{\widehat{\lambda}, med}(s) \} \{ \widehat{\Delta}_{CF}^{\widehat{\lambda}, r}(t) - \widehat{\Delta}_{CF}^{\widehat{\lambda}, med}(t) \}$, where $\widehat{\Delta}_{CF}^{\widehat{\lambda}, r}$ is given at the end of Section 3.3, and \widehat{C}^r is the estimated covariance for $\widehat{\Delta}_{CF}^{\widehat{\lambda}, r}$ as per Remark 6. Let \widehat{r} be the index of \widetilde{C}^r whose operator norm is a median among $\widetilde{C}^1, \dots, \widetilde{C}^R$. Then we use $\widetilde{C}^{\widehat{r}}$ as the estimate of the covariance function of $\widehat{\Delta}_{CF}^{\widehat{\lambda}, med}$.

5 Simulation Studies

Our simulation data consist of n independent samples from the joint distribution of (X, A, Y) . The confounder X follows a uniform distribution on $[-1, 1]$. Conditional on X , the treatment A follows a Bernoulli distribution with mean $P(A = 1 | X) = \text{expit}(1 + X)$, where $\text{expit}(\cdot) = \exp(\cdot)/(1 + \exp(\cdot))$. The outcome Y , which is a random distribution function, is generated through the corresponding quantile function $Y^{-1}(\alpha) = (-\mathbb{E}(A) + A + X + \epsilon) \sin(\pi\alpha)/8 + \alpha$, $\alpha \in [0, 1]$, where ϵ is independently generated from a uniform distribution on $[-0.5, 0.5]$. Note that for any realization of X and A , $Y^{-1}(0) = 0$, $Y^{-1}(1) = 1$, and $Y^{-1}(\alpha)$ is a continuous and strictly increasing function of α , so that Y^{-1} is a quantile function for a continuous random variable taking values in $\mathcal{I} = [0, 1]$. It follows that $Y \in \mathcal{W}_2(\mathcal{I})$. We are interested in estimating the causal effect at the reference distribution μ_0 , whose true value is $\Delta^{\mu_0}(t) = \sin(\pi t)/8$, $t \in \mathcal{I}$.

The sample sizes are $n = 50, 200, 1000$. For each subject $i = 1, \dots, n$, we assume that we have access to 1001 independent and identically distributed observations sampled from the distribution function $Y_i(t)$, $t \in [0, 1]$. We estimated the outcomes $Y_i(t)$ by the empirical cumulative distribution function $\widehat{Y}_i(t)$ based on these observations.

We considered two specifications for the outcome regression model: a linear regression model with predictor X in $m_A(X)$ (correct) and one with predictor X^2 (incorrect), and two specifications for the propensity score model: a logistic regression model with predictor X (correct) and one with predictor X^2 (incorrect). The estimation error is quantified using two measures: (1) bias of difference in medians, i.e., $\widehat{\Delta}^{\widehat{\mu}_0}(\widehat{\mu}_0^{-1}(0.5)) - \Delta^{\mu_0}(\mu_0^{-1}(0.5))$; (2) root mean integrated squared error under the reference distribution μ_0 , i.e., $\|\widehat{\Delta}^{\widehat{\mu}_0} \circ \widehat{\mu}_0^{-1} \circ \mu_0 - \Delta^{\mu_0}\|_{\mu_0}$.

To illustrate double robustness of the estimators $\widehat{\Delta}_{DR}^{\widehat{\mu}_0}$ and $\widehat{\Delta}_{CF}^{\widehat{\mu}_0, med}$, we compare them with the inverse probability weighting (IPW) and outcome regression (OR) estimators, defined by $\widehat{\Delta}_{OR}^{\widehat{\mu}_0} = \sum_{a=0,1} (2a - 1) \mathbb{P}_n \widehat{m}_a^{\widehat{\mu}_0}(X)$ and $\widehat{\Delta}_{IPW}^{\widehat{\mu}_0} = \sum_{a=0,1} (2a - 1) \mathbb{P}_n I(A = a)(\widehat{Y}^{-1} \circ \widehat{\mu}_0)/\widehat{f}(A | X)$. The cross-fitting estimator $\widehat{\Delta}_{CF}^{\widehat{\mu}_0, med}$ is based on the median of cross-fitting estimators from 100 random splits, where for each random split, we consider the 5-fold cross-fitting.

Table 1 summarizes the simulation results based on 1000 Monte Carlo replicates. The bias of difference in medians of the doubly robust estimator becomes closer to zero as the sample size increases when either the outcome regression or propensity score model is correct, thus confirming “double robustness.” In comparison, neither the OR nor IPW estimator has the double robustness property: When the corresponding model is misspecified, their bias of difference in medians can be large even with a sample size of 1000. Similar results hold for root mean integrated squared error. We further note that when the outcome resides in a Euclidean space, it is well-known that when both models are correct, the standard error of the

OR estimator is no larger than that of the DR estimator, which is in turn no larger than that of the IPW estimator. One can see a similar phenomenon from Table 1, where the outcome is a random distribution function residing in $\mathcal{W}_2(\mathcal{I})$. Although the cross-fitting estimator $\widehat{\Delta}_{CF}^{\mu_0, med}$ is more appealing theoretically, for the setting we consider here, $\widehat{\Delta}_{DR}^{\mu_0}$ has better finite sample performance, especially when the sample size is small.

We assess the finite-sample coverage of the proposed confidence bands in Remark 7 when both models are correctly specified. For the DR method, the coverage probabilities of the 95% SCB are 88.4%, 91.5%, and 92.4%, respectively for $n = 50, 200, 1000$, based on 1000 Monte Carlo replicates. For the CF method, the coverage probabilities are 80.8%, 91.4%, and 92.4%, respectively for $n = 50, 200, 1000$. These coverage probabilities are reasonably close to the nominal level considering the difficulty to derive effective confidence bands for functional objects.

We further consider the data-adaptive DR and CF estimators for two scenarios. Scenario 1 is exactly the same as the previous simulation. In Scenario 2, both the propensity score model and the outcome regression model are nonlinear functions of X . In particular, we set $P(A = 1 | X) = \text{expit}(1 + \sin(\pi X))$ and $Y^{-1}(\alpha) = (-\mathbb{E}(A) + A + \sin(\pi X) + \epsilon) \sin(\pi \alpha) / 8 + \alpha$, $\alpha \in [0, 1]$, i.e. we replace the term X in these two models by $\sin(\pi X)$. The remaining settings are the same as those in Scenario 1. In both scenarios, we fit the outcome regression model using smoothing spline, implemented by the R function `smooth.spline`, while for the propensity score model, we consider the logistic smoothing spline fit, implemented by the R function `gssanova` in package `gss`. The default tuning methods of these R functions are adopted, namely, generalized cross-validation for `smooth.spline` and cross-validation for `gssanova`; see the corresponding R packages for more details. The results based on 1000 Monte Carlo replicates are summarized in Table 2. From the results, one can see that for Scenario 1, the data-adaptive methods work reasonably well, although not as good as the method where we correctly specify both the outcome and propensity score models parametrically. When both the underlying true outcome and propensity score models are nonlinear, the root mean integrated squared errors of the data-adaptive methods decay as the sample size increases, suggesting consistency of these methods for estimating the average treatment effect.

6 Data Application

Behavioral scientists are often interested in evaluating the effects of potential risk factors, such as marriage, on physical activity patterns (e.g. King et al., 1998). In this section, we apply our proposed method to estimate the causal effect of marriage on physical activity levels, with data

Table 1: Bias of difference in medians $\times 100$ (standard error $\times 100$) and root mean integrated squared error $\times 100$ (standard error $\times 100$) of four proposed estimators: the outcome regression estimator $\widehat{\Delta}_{OR}^{\mu_0}$, the inverse probability weighting estimator $\widehat{\Delta}_{IPW}^{\mu_0}$, the doubly robust estimator $\widehat{\Delta}_{DR}^{\mu_0}$, and the cross-fitting estimator $\widehat{\Delta}_{CF}^{\mu_0, med}$

Estimator	Model		Sample size		
	PS	OR	$n = 50$	$n = 200$	$n = 1000$
Bias of difference in medians $\times 100$					
$\widehat{\Delta}_{OR}^{\mu_0}$	-	✓	0.010(0.037)	-0.036(0.018)	0.008(0.008)
$\widehat{\Delta}_{OR}^{\mu_0}$	-	×	3.898(0.075)	3.787(0.037)	3.819(0.017)
$\widehat{\Delta}_{IPW}^{\mu_0}$	✓	-	0.433(0.157)	0.008(0.045)	0.021(0.018)
$\widehat{\Delta}_{IPW}^{\mu_0}$	×	-	3.975(0.084)	3.706(0.036)	3.738(0.016)
$\widehat{\Delta}_{DR}^{\mu_0}$	✓	✓	0.005(0.04)	-0.033(0.019)	0.013(0.008)
$\widehat{\Delta}_{DR}^{\mu_0}$	✓	×	0.194(0.057)	-0.001(0.022)	0.020(0.010)
$\widehat{\Delta}_{DR}^{\mu_0}$	×	✓	0.015(0.038)	-0.038(0.018)	0.009(0.008)
$\widehat{\Delta}_{DR}^{\mu_0}$	×	×	3.881(0.074)	3.704(0.036)	3.737(0.016)
$\widehat{\Delta}_{CF}^{\mu_0, med}$	✓	✓	-0.066(0.091)	-0.032(0.019)	0.013(0.008)
$\widehat{\Delta}_{CF}^{\mu_0, med}$	✓	×	-2.151(0.141)	-0.383(0.025)	-0.051(0.010)
$\widehat{\Delta}_{CF}^{\mu_0, med}$	×	✓	0.014(0.047)	-0.038(0.018)	0.009(0.008)
$\widehat{\Delta}_{CF}^{\mu_0, med}$	×	×	4.193(0.108)	3.726(0.036)	3.741(0.016)
Root mean integrated squared error $\times 100$					
$\widehat{\Delta}_{OR}^{\mu_0}$	-	✓	0.695(0.016)	0.339(0.008)	0.150(0.003)
$\widehat{\Delta}_{OR}^{\mu_0}$	-	×	2.941(0.05)	2.773(0.027)	2.796(0.012)
$\widehat{\Delta}_{IPW}^{\mu_0}$	✓	-	2.912(0.108)	0.981(0.029)	0.425(0.009)
$\widehat{\Delta}_{IPW}^{\mu_0}$	×	-	3.176(0.057)	2.715(0.026)	2.736(0.012)
$\widehat{\Delta}_{DR}^{\mu_0}$	✓	✓	0.740(0.017)	0.348(0.008)	0.156(0.004)
$\widehat{\Delta}_{DR}^{\mu_0}$	✓	×	0.991(0.028)	0.409(0.010)	0.183(0.004)
$\widehat{\Delta}_{DR}^{\mu_0}$	×	✓	0.709(0.016)	0.342(0.008)	0.150(0.003)
$\widehat{\Delta}_{DR}^{\mu_0}$	×	×	2.942(0.048)	2.712(0.026)	2.736(0.012)
$\widehat{\Delta}_{CF}^{\mu_0, med}$	✓	✓	0.981(0.054)	0.352(0.008)	0.156(0.004)
$\widehat{\Delta}_{CF}^{\mu_0, med}$	✓	×	2.163(0.107)	0.495(0.013)	0.188(0.004)
$\widehat{\Delta}_{CF}^{\mu_0, med}$	×	✓	0.834(0.047)	0.343(0.008)	0.150(0.003)
$\widehat{\Delta}_{CF}^{\mu_0, med}$	×	×	3.289(0.070)	2.728(0.026)	2.738(0.012)

Table 2: Bias of difference in medians $\times 100$ (standard error $\times 100$) and root mean integrated squared error $\times 100$ (standard error $\times 100$) of data-adaptive doubly robust estimator $\widehat{\Delta}_{DRA}^{\mu_0}$ and the data-adaptive cross-fitting estimator $\widehat{\Delta}_{CFA}^{\mu_0, med}$

Estimator	Scenario	Sample size		
		$n = 50$	$n = 200$	$n = 1000$
Bias of difference in medians $\times 100$				
$\widehat{\Delta}_{DRA}^{\mu_0}$	1	-0.047(0.127)	-0.096(0.046)	0.012(0.008)
$\widehat{\Delta}_{DRA}^{\mu_0}$	2	-0.205(0.139)	-0.010(0.042)	0.030(0.008)
$\widehat{\Delta}_{CFA}^{\mu_0}$	1	-2.505(0.534)	-0.469(0.035)	-0.102(0.011)
$\widehat{\Delta}_{CFA}^{\mu_0}$	2	-1.206(0.788)	-0.808(0.122)	0.180(0.021)
Root mean integrated squared error $\times 100$				
$\widehat{\Delta}_{DRA}^{\mu_0}$	1	1.604(0.091)	0.545(0.044)	0.156(0.004)
$\widehat{\Delta}_{DRA}^{\mu_0}$	2	1.867(0.096)	0.686(0.153)	0.161(0.004)
$\widehat{\Delta}_{CFA}^{\mu_0}$	1	3.648(0.355)	0.767(0.024)	0.244(0.006)
$\widehat{\Delta}_{CFA}^{\mu_0}$	2	5.111(0.894)	2.202(0.183)	0.568(0.012)

obtained from the National Health and Nutrition Examination Survey (NHANES) 2005-2006¹. The NHANES is a program of studies designed to assess the health and nutritional status of adults and children in the United States. The survey is unique in that it combines interviews and physical examinations. The NHANES interview includes demographic, socioeconomic, dietary, and health-related questions. The examination component consists of medical, dental, and physiological measurements, as well as laboratory tests administered by highly trained medical personnel.

In the 2005-2006 cycle of NHANES, participants of ages six years and older were asked to wear an Actigraph 7164 on a waist belt during all non-sleeping hours for seven days. The technology and application of current accelerometer-based devices in physical activity research allow the capture and storage or transmission of large volumes of raw acceleration signal data (Troiano et al., 2014). The NHANES accelerometer data have been widely used by researchers to explore relationships among accelerometer measures and a variety of other measures (e.g. Tudor-Locke et al., 2012). The monitors were programmed to begin recording activity information for successive 1-minute intervals (epochs) beginning at 12:01 a.m. the day after the health examination. The device was placed on an elasticized fabric belt, custom-fitted for each subject,

¹<https://wwwn.cdc.gov/nchs/nhanes/ContinuousNhanes/Default.aspx?BeginYear=2005>.

and worn on the right hip. Subjects were told to keep the device dry (i.e. remove it before swimming or bathing) and to remove the device at bedtime. For each participant, the physical activity intensity, ranging from 0 to 32767 counts per minute (cpm), was recorded every minute for 24 hours, 7 days, where 32767 is the maximum value that the wearable device can record.

In our analysis, the exposure of interest is marriage, coded as a binary variable, with 1 being married or living with a partner, and 0 being otherwise. To define the outcome variable, we note that the trajectory of activity intensity is not directly comparable across different subjects as different individuals might have different circadian rhythms. Instead, the distribution of activity intensity is invariant to circadian rhythms and hence can be compared between groups of individuals. Specifically, our outcome of interest is $Y(s) = \text{Leb}(\{t : Z(t) \leq s\})/7$, the distribution of physical activity intensity over 7 days, where Leb denotes the Lebesgue measure.

To obtain robust and reliable results, we applied the following preprocessing steps. Firstly, we excluded all observations that data reliability is questionable following NHANES protocol, after which there were 7170 subjects left. Secondly, following Chang and McKeague (2020), for each subject, we removed observations with intensity values higher than 1000 or equal to 0. In the data set, most intensity values are between 0 and 1000 cpm. Observations with zero intensity value were removed as they could represent activities with very different intensities, such as sleeping, bathing and swimming. Thirdly, we removed subjects with no more than 100 observations left, which further reduced the sample size to 7014. Lastly, for illustrative purposes, we removed 1490 participants for whom we do not have information on their marital status.

After the preprocessing steps, we are left with 5524 participants in the data set, among which 2682 are in the married group and 2842 participants are in the unmarried group. The average age was 40.2 years old with a standard deviation of 21.3, and 52.3% of them were female. As an example of the outcome data, in Figure 2(a), we plot the empirical cumulative distribution function for a randomly selected participant (subject ID 31144) who was 21 years old, male, and unmarried. In Figure 2(b), we plot the Wasserstein barycentres of the empirical cumulative distribution functions in the married group and unmarried group, respectively. One can see that the Wasserstein barycentres retain the key structural information in the individual empirical CDFs. For example, their derivatives decrease with the intensity level, suggesting that the physical intensity level is low most of the time. The Wasserstein barycentre in the married group is stochastically greater than that in the unmarried group, suggesting a positive association between marriage and physical activity level. However, this crude association may be subject to potential confounders such as age and gender.

A simple approach to answering our question of interest is to first summarize the distribution

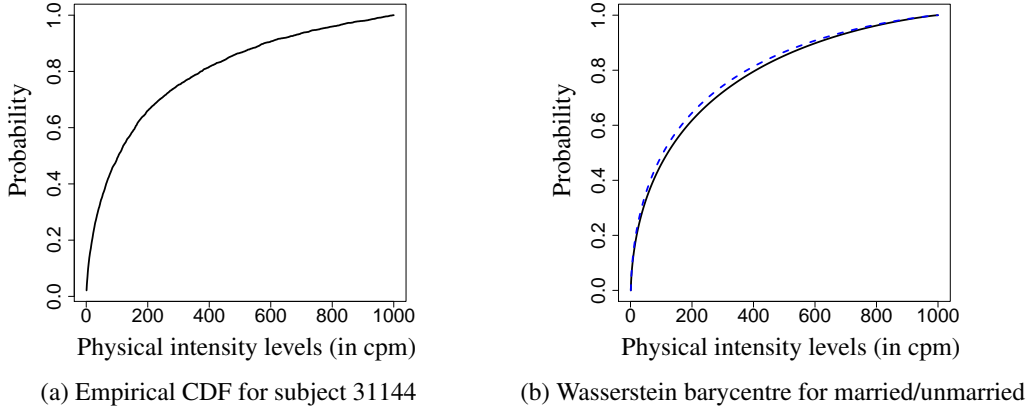


Figure 2: Panel (a) plots the preprocessed data for a randomly selected subject, where we transform the raw trajectory data to a cumulative distribution function in $\mathcal{W}_2([1, 1000])$. Panel (b) plots the Wasserstein barycentre of the empirical cumulative distribution functions in the married group (black solid line) and unmarried group (blue dashed line).

functions with their means and then apply standard approaches such as the doubly robust estimator of Robins et al. (1994) to estimate the causal effect. With a linear outcome regression model and a logistic propensity score model, this simple doubly robust approach suggests that marriage increases the average physical intensity by 21.7 (95% CI = [17.1, 26.3]) cpm.

We then present a finer analysis of these data with the proposed approaches. We first plot the estimates of causal Wasserstein barycentres, $\widehat{\mu}_1$ and $\widehat{\mu}_0$ by OR, DR, and CF in Figure 3. Here, for $a = 0, 1$, $\widehat{\mu}_a$ is the corresponding cumulative distribution function of the estimate $\widehat{\mu}_a^{-1} = \widehat{\mu}_a^{-1, \widehat{\lambda}} \circ \widehat{\lambda}^{-1}$ for μ_a^{-1} , where for the OR method, $\widehat{\mu}_a^{-1, \widehat{\lambda}} = \mathbb{P}_n \widehat{m}_a^{\widehat{\lambda}}(X)$, for the DR method, $\widehat{\mu}_a^{-1, \widehat{\lambda}}$ is defined in (8), and for the CF method, in the spirit of (10), $\widehat{\mu}_a^{-1} = \text{median}\{\widehat{\mu}_{a, CF}^{-1, \widehat{\lambda}, r}\}_{r=1}^R$ with $\widehat{\mu}_{a, CF}^{-1, \widehat{\lambda}, r}$ being the estimator in (9) for the r th partitioning. With these estimators, the former is stochastically greater than the latter, suggesting that marriage improves the entire distribution of physical intensity level at every quantile.

To quantify the size of the treatment effect, we take the difference between $\widehat{\mu}_1^{-1}$ and $\widehat{\mu}_0^{-1}$, corresponding to the difference in quantiles of the mean potential outcomes μ_1 and μ_0 . To quantify the uncertainty of these estimates, we plot the corresponding 95% confidence bands in Figure 4 (b)–(d), where the confidence bands for the doubly robust and cross-fitting estimators were obtained using our asymptotic results presented in Theorems 3 and 4, and the confidence band for the outcome regression estimator was obtained using the conventional linear regression confidence interval for the slope coefficient corresponding to the exposure A . As expected, the estimation results from the three methods are very close to each other, and the OR method has

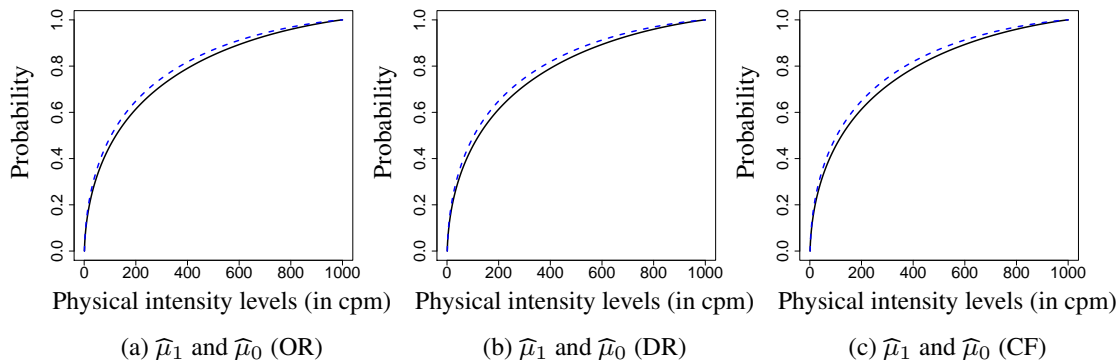


Figure 3: Panel (a), (b) and (c) plots $\hat{\mu}_1$ (black solid line) and $\hat{\mu}_0$ (blue dashed line) estimated by OR, DR and CF, respectively.

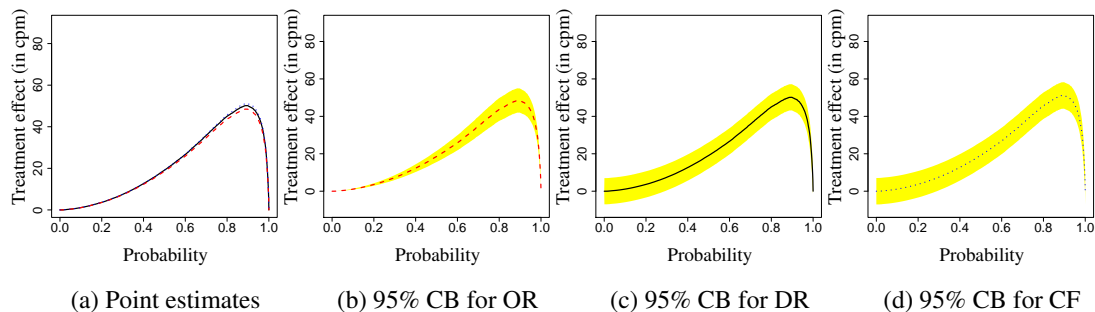


Figure 4: Difference in quantiles estimates with the OR (red dashed), DR (black solid) and CF (blue dotted) estimators: point estimates and 95% confidence bands.

the tightest confidence band among the three methods.

One can see from Figure 4 that the effect of marriage on physical activity level is significant at the 0.05 level. One can also get the causal effect on individual quantiles from these plots. For example, according to the DR estimation results, on average, marriage improves the median physical intensity level by 19.1 (95% CI = [12.1, 26.1]) cpm. Due to Theorem 1, this effect may be interpreted on both the population and individual levels. On the population level, this means that marriage improves the median of “average” (in the sense of Wasserstein barycentre) physical intensity level by 19.1 cpm. On the individual level, this means that the average improvement on the median physical intensity level is 19.1 cpm. We also estimate the Wasserstein distance between $\hat{\mu}_1^{DR}, \hat{\mu}_0^{DR}$, $W_2(\hat{\mu}_1^{DR}, \hat{\mu}_0^{DR}) = \|\hat{\Delta}_{\hat{\mu}_0^{DR}, DR}\|_{\hat{\mu}_0^{DR}}$, and the estimate is 27.6 cpm (95% CI: [24.0, 31.2]).

One may also be interested in predicting the unobserved potential outcome for a particular individual. As an illustration, we estimate $Y_i(1)$ for Subject 31144, who was unmarried so

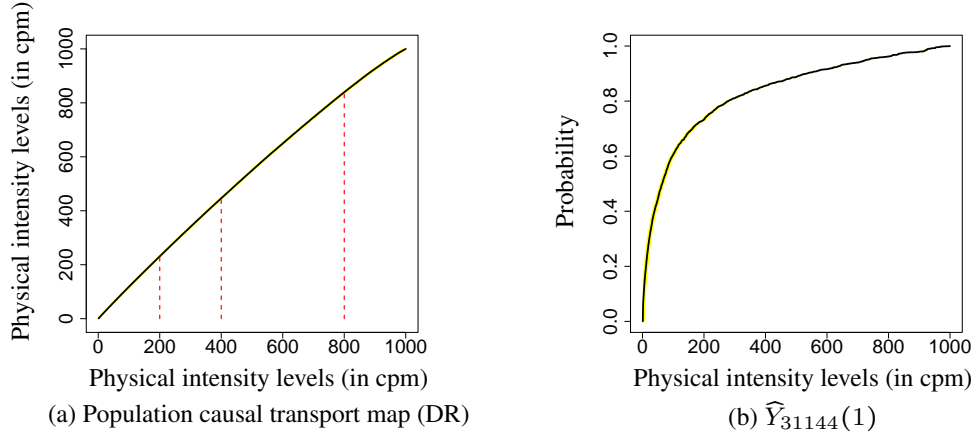


Figure 5: Panel (a) plots the DR estimate of population causal transport map, superimposed with the 95% confidence band; Panel (b) plots the DR estimate of counterfactual outcome $Y(1)$ with 95% confidence band for individual 31144, who was unmarried so that $Y_{31144} = Y_{31144}(0)$.

$Y_{31144} = Y_{31144}(0)$. Recall that $\Delta_i^{Y_i(0)} = T_i - \text{id}$. We first estimate the individual causal effect map for Subject 31144 using the average causal effect map with reference distribution $\widehat{Y}_{31144} : \widehat{T}_{31144} = \widehat{\Delta}^{\widehat{Y}_{31144}} + \text{id}$, the latter being estimated using the DR method. We then apply the individual causal transport map to his empirical CDF to obtain $\widehat{Y}_{31144}(1)$ plotted in Figure 5(b). From this, one may obtain, for example, getting married would raise his mean physical activity from 144.5 cpm to 166.3 cpm (95% CI: [159.5, 173.7]).

We also compare our adjusted estimates with the results where we do not adjust for the observed confounders age and gender. In particular, we apply the OR, DR, and CF estimators for estimating the average treatment effect Δ^λ . We plot these estimates and the corresponding 95% confidence bands in Figure 6. One can see the treatment effect is attenuated without adjusting for age and gender.

7 Discussion

In this paper, we study causal inference for distribution functions that reside in a Wasserstein space. We propose novel definitions of causal effects and develop doubly robust estimation procedures for estimating these effects under the assumption of no unmeasured confounding. It would be interesting to extend classical causal inference methods for dealing with unmeasured confounding, such as the instrumental variable methods (e.g. Ogburn et al., 2015; Wang and Tchetgen Tchetgen, 2018) to this setting.

To the best of our knowledge, ours is the first formal study of causal effects for outcomes

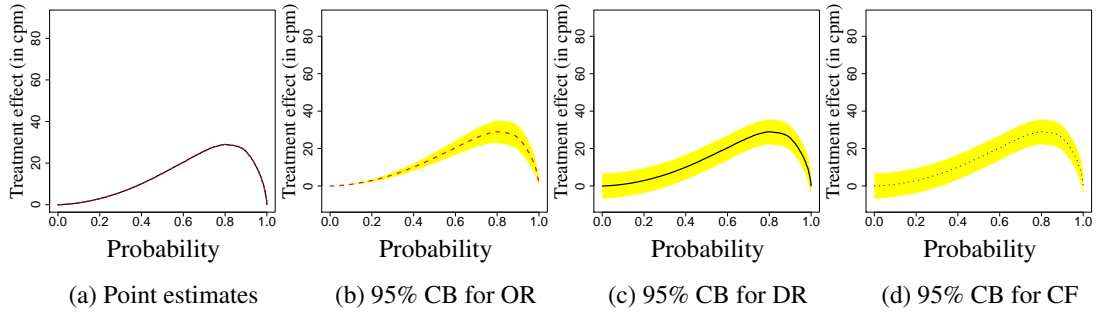


Figure 6: Difference in quantiles estimates with the OR (red dashed), DR (black solid) and CF (blue dotted) estimators when we do not adjust for observed confounders age and gender: point estimates and 95% confidence bands.

defined in a non-linear space. As such, we have only considered a leading special case of non-linear spaces. There are many other data objects from non-linear spaces that we do not consider in this paper. For example, the Wasserstein spaces of probability distributions on higher dimensional Euclidean spaces exhibit structures different from $\mathcal{W}_2(\mathcal{I})$ and thus pose new challenges for causal inference on such spaces. We also note that although the Wasserstein space $\mathcal{W}_2(\mathcal{I})$ is not a Riemannian manifold (Bigot et al., 2017), it can be endowed with a Riemannian structure, including the tangent space and Riemannian logarithmic map. In particular, let $cl(S)$ denote the closure of set S . With a continuous reference distribution λ , the space $T_\lambda \mathcal{W}_2(\mathcal{I}) = cl\{k(v^{-1} \circ \lambda - id) : v \in \mathcal{W}_2(\mathcal{I}), k \in \mathbb{R}^+\}$ can be viewed as the tangent space of $\mathcal{W}_2(\mathcal{I})$ at λ , and the mapping $v \mapsto v^{-1} \circ \lambda - id$ can be viewed as the Riemannian logarithmic map at λ (Ambrosio et al., 2004). From this perspective, with the notation $\mathcal{L}_\lambda v = v^{-1} \circ \lambda$, the individual causal effect maps can be written as $\Delta_i^\lambda = \mathcal{L}_\lambda Y_i(1) - \mathcal{L}_\lambda Y_i(0) = \{\mathcal{L}_\lambda Y_i(1) - id\} - \{\mathcal{L}_\lambda Y_i(0) - id\}$, so they may be equivalently defined as the contrasts between the Riemannian logarithmic maps of distribution functions $Y_i(1)$ and $Y_i(0)$. By Theorem 1, the average causal effect map may then be equivalently defined as $\Delta^\lambda = \mathbb{E}(\mathcal{L}_\lambda Y(1) - id) - \mathbb{E}(\mathcal{L}_\lambda Y(0) - id)$. These connections allow one to extend the proposed definition of causal effect from random distributions to random elements residing on a Riemannian manifold; see Srivastava and Klassen (2016) for concepts and tools of Riemannian manifolds that are relevant to statistics.

Another interesting venue for future research is the study of efficiency theory with distribution-valued outcomes. It is well-known that the classical doubly robust and cross-fitting estimators (Robins et al., 1994; Chernozhukov et al., 2018) are both doubly robust and locally semiparametric efficient. In Theorems 3 and 4 we establish double robustness of our proposed doubly robust and cross-fitting estimators. On the other hand, to establish semiparametric efficiency of these proposed estimators, one needs to extend semiparametric efficiency theory to accommodate

distribution-valued outcomes that reside in infinite-dimensional functional spaces. This will be developed in a separate paper.

Supplementary Material

The supplementary file contains some auxiliary results, technical lemmas, and proofs for all the theorems. R code to reproduce the simulation studies and data analysis can be found in the repository <https://github.com/kongdehanstat/causaldistributionfunction>. The data analyzed in Section 6 is available at <https://wwwn.cdc.gov/nchs/nhanes/ContinuousNhanes/Default.aspx?BeginYear=2005>.

References

- Agueh, M. and Carlier, G. (2011), “Barycenters in the Wasserstein space,” *SIAM Journal on Mathematical Analysis*, 43, 904–924.
- Ambrosio, L., Gigli, N., and Savaré, G. (2004), “Gradient flows with metric and differentiable structures, and applications to the Wasserstein space,” *Atti della Accademia Nazionale dei Lincei. Classe di Scienze Fisiche, Matematiche e Naturali. Rendiconti Lincei. Serie IX. Matematica e Applicazioni*, 15, 327–343.
- Ambrosio, L., Gigli, N., and Savaré, G. (2005), *Gradient Flows*, Birkhäuser Basel.
- Arjovsky, M., Chintala, S., and Bottou, L. (2017), “Wasserstein generative adversarial networks,” in *International Conference on Machine Learning*, PMLR, pp. 214–223.
- Bernton, E., Jacob, P. E., Gerber, M., and Robert, C. P. (2019), “Approximate Bayesian computation with the Wasserstein distance,” *Journal of the Royal Statistical Society: Series B (Statistical Methodology)*, 81, 235–269.
- Bigot, J. (2020), “Statistical data analysis in the Wasserstein space,” *ESAIM: Proceedings and Surveys*, 68, 1–19.
- Bigot, J., Gouet, R., Klein, T., and López, A. (2017), “Geodesic PCA in the Wasserstein space by convex PCA,” *Annales de l’Institut Henri Poincaré, Probabilités et Statistiques*, 53, 1–26.
- Bigot, J., Imb, T. K., Imt, and Enac (2012), “Characterization of barycenters in the Wasserstein space by averaging optimal transport maps,” *Esaim: Probability and Statistics*, 22, 35–57.

- Chang, H.-W. and McKeague, I. W. (2020), “Nonparametric comparisons of activity profiles from wearable device data,” *preprint*.
- Chen, Y., Lin, Z., and Müller, H.-G. (2021), “Wasserstein regression,” *Journal of the American Statistical Association*, 1–14.
- Chernozhukov, V., Chetverikov, D., Demirer, M., Duflo, E., Hansen, C., Newey, W., and Robins, J. (2018), “Double/debiased machine learning for treatment and structural parameters,” *The Econometrics Journal*, 21, C1–C68.
- Courty, N., Flamary, R., Tuia, D., and Rakotomamonjy, A. (2016), “Optimal transport for domain adaptation,” *IEEE Transactions on Pattern Analysis and Machine Intelligence*, 39, 1853–1865.
- Cuturi, M. and Doucet, A. (2014), “Fast computation of Wasserstein barycenters,” *Proceedings of the 31st International Conference on Machine Learning (ICML)*, 32.
- del Barrio, E., Cuesta-Albertos, J. A., Matrán, C., and Rodríguez-Rodríguez, J. M. (1999), “Tests of goodness of fit based on the L2-Wasserstein distance,” *Annals of Statistics*, 1230–1239.
- Evans, S. N. and Matsen, F. A. (2012), “The phylogenetic Kantorovich–Rubinstein metric for environmental sequence samples,” *Journal of the Royal Statistical Society: Series B (Statistical Methodology)*, 74, 569–592.
- Fournier, N. and Guillin, A. (2015), “On the rate of convergence in Wasserstein distance of the empirical measure,” *Probability Theory and Related Fields*, 162, 707–738.
- Hernán, M. and Robins, J. (2020), *Causal Inference: What If*, Chapman & Hall/CRC.
- Ho, N., Nguyen, X., Yurochkin, M., Bui, H. H., Huynh, V., and Phung, D. (2017), “Multilevel clustering via Wasserstein means,” in *International Conference on Machine Learning*, PMLR, pp. 1501–1509.
- Kim, Y.-H. and Pass, B. (2017), “Wasserstein barycenters over Riemannian manifolds,” *Advances in Mathematics*, 307, 640–683.
- King, A. C., Kiernan, M., Ahn, D. K., and Wilcox, S. (1998), “The effects of marital transitions on changes in physical activity: results from a 10-year community study,” *Annals of Behavioral Medicine*, 20, 64–69.

- Kuelbs, J. (1978), “Some Exponential Moments of Sums of Independent Random Variables,” *Transactions of the American Mathematical Society*, 240, 145–162.
- Mammen, E. and van de Geer, S. (1997), “Locally adaptive regression splines,” *Annals of Statistics*, 25, 387–413.
- Neyman, J. S. (1923), “On the application of probability theory to agricultural experiments. essay on principles. section 9.(translated and edited by dm dabrowska and tp speed, statistical science (1990), 5, 465-480),” *Annals of Agricultural Sciences*, 10, 1–51.
- Ogburn, E. L., Rotnitzky, A., and Robins, J. M. (2015), “Doubly robust estimation of the local average treatment effect curve,” *Journal of the Royal Statistical Society: Series B (Statistical Methodology)*, 77, 373–396.
- Panaretos, V. M. and Zemel, Y. (2019), “Statistical aspects of Wasserstein distances,” *Annual Review of Statistics and Its Application*, 6, 405–431.
- Petersen, A. and Müller, H.-G. (2016), “Functional data analysis for density functions by transformation to a Hilbert space,” *The Annals of Statistics*, 44, 183–218.
- Petersen, A. and Müller, H.-G. (2019), “Fréchet Regression for Random Objects with Euclidean Predictors,” *The Annals of Statistics*, 47, 691–719.
- Ramsay, J. O. and Silverman, B. W. (2005), *Functional Data Analysis*, Springer.
- Robins, J. M., Rotnitzky, A., and Zhao, L. P. (1994), “Estimation of regression coefficients when some regressors are not always observed,” *Journal of the American Statistical Association*, 89, 846–866.
- Rosenbaum, P. R. and Rubin, D. B. (1983), “The central role of the propensity score in observational studies for causal effects,” *Biometrika*, 70, 41–55.
- Rubin, D. B. (1974), “Estimating causal effects of treatments in randomized and nonrandomized studies.” *Journal of Educational Psychology*, 66, 688.
- (1980), “Comment,” *Journal of the American Statistical Association*, 75, 591–593.
- Santambrogio, F. (2015), *Optimal Transport for Applied Mathematicians*, Birkhäuser Basel.
- Schiebinger, G., Shu, J., Tabaka, M., Cleary, B., Subramanian, V., Solomon, A., Gould, J., Liu, S., Lin, S., Berube, P., Lee, L., Chen, J., Brumbaugh, J., Rigollet, P., Hochedlinger, K.,

- Jaenisch, R., Regev, A., and Lander, E. S. (2019), “Optimal-Transport Analysis of Single-Cell Gene Expression Identifies Developmental Trajectories in Reprogramming,” *Cell*, 176, 928–943.
- Schötz, C. (2019), “Convergence rates for the generalized Fréchet mean via the quadruple inequality,” *Electronic Journal of Statistics*, 13, 4280–4345.
- Sommerfeld, M. and Munk, A. (2018), “Inference for empirical Wasserstein distances on finite spaces,” *Journal of the Royal Statistical Society: Series B (Statistical Methodology)*, 80, 219–238.
- Srivastava, A. and Klassen, E. P. (2016), *Functional and shape data analysis*, vol. 1, Springer.
- Troiano, R. P., McClain, J. J., Brychta, R. J., and Chen, K. Y. (2014), “Evolution of accelerometer methods for physical activity research,” *British Journal of Sports Medicine*, 48, 1019–1023.
- Tudor-Locke, C., Camhi, S. M., and Troiano, R. P. (2012), “Peer reviewed: a catalog of rules, variables, and definitions applied to accelerometer data in the National Health and Nutrition Examination Survey, 2003–2006,” *Preventing Chronic Disease*, 9.
- van de Geer, S. (1990), “Estimating a regression function,” *Annals of Statistics*, 18, 907–924.
- van der Vaart, A. W. (1998), *Asymptotic Statistics*, Cambridge: Cambridge University Press.
- Verdinelli, I., Wasserman, L., et al. (2019), “Hybrid Wasserstein distance and fast distribution clustering,” *Electronic Journal of Statistics*, 13, 5088–5119.
- Villani, C. (2003), *Topics in optimal transportation*, no. 58, American Mathematical Soc.
- von Mering, C., Hugenholtz, P., Raes, J., Tringe, S., Doerks, T., Jenst, L., Ward, N., and Bork, P. (2007), “Quantitative phylogenetic assessment of microbial communities in diverse environments,” *Science*, 315, 1126–1130.
- Wang, L. and Tchetgen Tchetgen, E. (2018), “Bounded, efficient and multiply robust estimation of average treatment effects using instrumental variables,” *Journal of the Royal Statistical Society: Series B (Statistical Methodology)*, 80, 531–550.
- Zhang, C., Kokoszka, P., and Petersen, A. (2020), “Wasserstein Autoregressive Models for Density Time Series,” *arXiv preprint arXiv:2006.12640*.

Zhou, H., Lin, Z., and Yao, F. (2021), “Intrinsic Wasserstein Correlation Analysis,” *arxiv*.

Zhu, C. and Müller, H.-G. (2021), “Autoregressive optimal transport models,” *arxiv*.

Supplementary Material for “Causal Inference on Distribution Functions”

Abstract

The supplementary file contains additional examples, some auxiliary results, technical lemmas and proofs for all the theorems.

1 Additional Motivating Examples

Example 2 (Cellular Differentiation). *In developmental biology, scientists are often interested in how an exposure influences the cellular differentiation process. In these studies, multiple samples of tissues may be collected in the exposure and control groups. For each sample, one randomly selects a set of cells and measures the expression level for $p \geq 1$ genes in these cells. This process is then repeated over a period of time. To understand molecular programs related to cell differentiation, in a high-profile work, Schiebinger et al. (2019) developed a so-called Waddington-OT framework based on the Wasserstein geometry. Under this framework, at each time point t , a sample is represented by a p -dimensional distribution \mathcal{P}_t of gene expression level over a population of cells. Typically these distributions are multi-modal, corresponding to different cell types in the samples. Experiment results in Schiebinger et al. (2019) suggest that cellular differentiation follows the shortest path under the Wasserstein geometry. In other words, one may use the Wasserstein geometry to reconstruct the differentiation path $\mathcal{P}_t, 0 \leq t \leq T$ with observations at time 0 and T .*

Example 3 (Metagenomics). *In microbial ecology, it is of interest to study whether an exposure changes the microbiome system in an environmental site (e.g., a human gut or acid mine drainage). To study this problem, multiple samples of microorganisms are collected from the environmental site in both control and exposure cohorts. For each sample, scientists use shotgun sequencing to obtain DNA sequences, and map each of the DNA sequence onto a node of a reference phylogenetic tree (von Mering et al., 2007). Consequently, a sample of microorganisms can be represented by an empirical distribution on a phylogenetic tree (Evans and Matsen, 2012). Such a distribution encodes both relative gene abundance and taxonomic information, which together characterize a microbiome system.*

2 Inference Based on Wasserstein Distance

It was suggested by a reviewer to provide estimation and inference details also for the Wasserstein distance $W_2(\mu_1, \mu_0)$ due to its simplicity, even though this quantity does not satisfy the desiderata (d). For this, by simple calculation or Lemma 1, we note that $W_2(\mu_1, \mu_0) = \|\Delta^\lambda\|_\lambda$ for any fixed continuous reference distribution λ . Therefore, it is intuitive to estimate $W_2(\mu_1, \mu_0)$ by $\|\hat{\Delta}_{DR}^\lambda\|_\lambda$ whose asymptotic distribution is provided below.

According to Theorem 3, $\sqrt{n}(\hat{\Delta}_{DR}^\lambda - \Delta^\lambda)$ converges weakly to a centered Gaussian process G in $L^2(\mathcal{J}; \lambda)$. Let $\phi(h) = \|h\|_\lambda^2$ for $h \in L^2(\mathcal{J}; \lambda)$. It is seen that its Hadamard derivative ϕ'_h (Section 20.2, van der Vaart, 1998) at h is $\phi'_h(g) = 2\langle g, h \rangle_\lambda$ for $g \in L^2(\mathcal{J}; \lambda)$. Then, according to Theorem 20.8 of van der Vaart (1998), $\sqrt{n}(\|\hat{\Delta}_{DR}^\lambda\|_\lambda^2 - \|\Delta^\lambda\|_\lambda^2)$ converges weakly to $2\langle \Delta^\lambda, G \rangle_\lambda$ which is a centered Gaussian (real-valued) random variable when $\Delta_{DR}^\lambda \neq 0$. In case of $\Delta_{DR}^\lambda = 0$, by continuous mapping theorem, $n\|\hat{\Delta}_{DR}^\lambda\|_\lambda^2$ converges weakly to $\|G\|_\lambda^2$. Based on these results, we can also derive the asymptotic distribution of $\sqrt{n}(\|\hat{\Delta}_{DR}^\lambda\|_\lambda - \|\Delta^\lambda\|_\lambda)$ by applying the delta method or continuous mapping theorem again. For example, $\sqrt{n}(\|\hat{\Delta}_{DR}^\lambda\|_\lambda - \|\Delta^\lambda\|_\lambda)$ converges weakly to the $N(0, \sigma^2\|\Delta^\lambda\|_\lambda^{-2})$ with $\sigma^2 = \text{var}(\langle \Delta^\lambda, G \rangle_\lambda)$ by the classic delta theorem when $\Delta^\lambda \neq 0$, and converges to $\|G\|_\lambda$ weakly by the continuous mapping theorem when $\Delta^\lambda = 0$.

The above results can be used to perform inference such as hypothesis tests on $W_2(\mu_1, \mu_0)$. For instance, to test the null hypothesis $W_2(\mu_1, \mu_0) = 0$, which is equivalent to $\|\Delta^\lambda\|_\lambda = 0$, we can use the test statistic $\sqrt{n}\|\hat{\Delta}_{DR}^\lambda\|_\lambda$, and reject the null hypothesis at the significance level α if it exceeds the $1 - \alpha$ quantile of $\|G\|_\lambda$. Such quantile can be estimated via resampling, as follows. As in Remark 6, we can obtain an estimate \hat{C} of the covariance function of G , and as in Remark 7, resample B (e.g., $B = 1000$) realizations G_1, \dots, G_B from the centered Gaussian process with the covariance function \hat{C} . For each realization we compute the norm $\|G_j\|_\lambda$ and finally estimate the $1 - \alpha$ quantile by the empirical $1 - \alpha$ quantile of $\|G_1\|_\lambda, \dots, \|G_B\|_\lambda$.

3 Remark on Condition Expectation in Assumption 3

The equation (11) involves conditional expectation of a random variable $W_2^2(\hat{Y}_i, Y_i)$ given a random distribution Y_i . Such conditional expectation is well defined, as follows. Underlying all random quantities is a probability space (Ω, \mathcal{E}, P) with a sample space Ω , an event space (σ -field) \mathcal{E} and a probability measure P . Both $Y_i : \Omega \rightarrow \mathcal{W}_2(\mathcal{I})$ and $\hat{Y}_i : \Omega \rightarrow \mathcal{W}_2(\mathcal{I})$ are measurable maps taking values in $\mathcal{W}_2(\mathcal{I})$, while $W_2^2(\hat{Y}_i, Y_i) : \Omega \rightarrow \mathbb{R}$ is a real-valued measurable map. Note that $\mathbb{E}\{W_2^2(\hat{Y}_i, Y_i)|Y_i\}$ is understood to be the conditional expectation $\mathbb{E}\{W_2^2(\hat{Y}_i, Y_i)|\sigma(Y_i)\}$ of the real random variable $W_2^2(\hat{Y}_i, Y_i)$ given the σ -field $\sigma(Y_i)$, where

$\sigma(Y_i) \subset \mathcal{E}$ is the smallest sub- σ -field that makes Y_i measurable. By the definition of conditional expectation given a sub- σ -field, $\mathbb{E}\{W_2^2(\widehat{Y}_i, Y_i)|\sigma(Y_i)\}$ is a measurable function, and further by the Doob–Dynkin lemma, there exists a measurable function $g : \mathcal{W}_2(\mathcal{I}) \rightarrow \mathbb{R}$ such that $\mathbb{E}\{W_2^2(\widehat{Y}_i, Y_i)|Y_i\} = \mathbb{E}\{W_2^2(\widehat{Y}_i, Y_i)|\sigma(Y_i)\} = g(Y_i)$. In the equation (11), $\mathbb{E}\{W_2^2(\widehat{Y}_i, Y_i)|Y_i = v\}$ represents $g(v)$, and thus is well defined.

4 Proof of Theorem 3

To simplify notation and unify the proofs, for probability distributions λ, ν , write $\mathcal{L}_\lambda \nu = \nu^{-1} \circ \lambda$ and

$$\tau_\lambda^\nu g = g \circ \lambda^{-1} \circ \nu \quad \text{for } g \in L^2(\mathcal{J}; \lambda). \quad (\text{S1})$$

Also, let $Z_i = \mathcal{L}_\lambda Y_i$, $\widehat{Z}_i = \mathcal{L}_{\widehat{\lambda}} \widehat{Y}_i$, $R_i = \tau_{\widehat{\lambda}}^\lambda \widehat{Z}_i - Z_i$, and $D_a(x) = \tau_{\widehat{\lambda}}^\lambda \widehat{m}_a^{\widehat{\lambda}}(x) - \widetilde{m}_a^\lambda(x)$. The quantity R_i can be viewed as the residual due to the discrepancy between $\widehat{\lambda}$ and λ , and between \widehat{Y}_i and Y_i . Define

$$\begin{aligned} \psi_1 &:= \mathbb{E} \left[\frac{A \mathcal{L}_\lambda Y}{\pi(X)} - \left\{ \frac{A}{\pi(X)} - 1 \right\} m_1^\lambda(X) \right], \\ \psi_0 &:= \mathbb{E} \left[\frac{(1-A) \mathcal{L}_\lambda Y}{1-\pi(X)} - \left\{ \frac{1-A}{1-\pi(X)} - 1 \right\} m_0^\lambda(X) \right] \end{aligned}$$

and their sample versions

$$\begin{aligned} \widehat{\psi}_1 &:= \mathbb{P}_n \left[\frac{A \mathcal{L}_{\widehat{\lambda}} \widehat{Y}}{\widehat{\pi}(X)} - \left\{ \frac{A}{\widehat{\pi}(X)} - 1 \right\} \widehat{m}_1^{\widehat{\lambda}}(X) \right], \\ \widehat{\psi}_0 &:= \mathbb{P}_n \left[\frac{(1-A) \mathcal{L}_{\widehat{\lambda}} \widehat{Y}}{1-\widehat{\pi}(X)} - \left\{ \frac{1-A}{1-\widehat{\pi}(X)} - 1 \right\} \widehat{m}_0^{\widehat{\lambda}}(X) \right]. \end{aligned}$$

Then we have $\Delta^\lambda = \psi_1 - \psi_0$ and $\widehat{\Delta}_{DR}^{\widehat{\lambda}} = \widehat{\psi}_1 - \widehat{\psi}_0$. In the above and in what follows, when $\widehat{\lambda} = \lambda$, the operator $\tau_{\widehat{\lambda}}^\lambda$ is an identity operator and has no effect. The proof will be based on the following decomposition for $\tau_{\widehat{\lambda}}^\lambda \widehat{\psi}_1$:

$$\begin{aligned} \tau_{\widehat{\lambda}}^\lambda \widehat{\psi}_1 - \psi_1 &= \mathbb{P}_n \left[\frac{AZ + AR}{\widehat{\pi}(X)} - \left\{ \frac{A}{\widehat{\pi}(X)} - 1 \right\} \{ \widetilde{m}_1^\lambda(X) + D_1(X) \} \right] - \psi_1 \\ &= \underbrace{(\mathbb{P}_n - \mathbb{E}_n) \left[\frac{A\{Z - \widetilde{m}_1^\lambda(X)\}}{\widehat{\pi}(X)} + \widetilde{m}_1^\lambda(X) - \frac{A\{Z - m_1^{\lambda,*}(X)\}}{\pi^*(X)} - m_1^{\lambda,*}(X) \right]}_I \end{aligned}$$

$$\begin{aligned}
& + \underbrace{(\mathbb{P}_n - \mathbb{E}_n) \left[\frac{A\{Z - m_1^{\lambda,*}(X)\}}{\pi^*(X)} + m_1^{\lambda,*}(X) \right]}_{\text{II}} \\
& + \underbrace{\mathbb{E}_n \left[\frac{\{\tilde{m}_1^\lambda(X) - m_1^\lambda(X)\}\{\hat{\pi}(X) - A\}}{\hat{\pi}(X)} \right]}_{\text{III}} \\
& + \underbrace{\mathbb{P}_n \left[\left\{ 1 - \frac{A}{\hat{\pi}(X)} \right\} D_1(X) \right]}_{\text{IV}} \\
& + \underbrace{\mathbb{P}_n \left\{ \frac{AR}{\hat{\pi}(X)} \right\}}_{\text{V}}.
\end{aligned}$$

Here, $\mathbb{E}_n(O) = n^{-1} \sum_{i=1}^n \mathbb{E}(O_i)$ for generic random quantities O_1, \dots, O_n . The decomposition for the other term is similar and thus omitted. In the sequel, we use c to denote a positive constant and allow its value to vary in different occurrences.

Proof of part (i). This is a direct consequence of Claims 1–5 and the assumed rates of α_n and ν_n . \square

Proof of part (ii). Under the assumed conditions, the terms I and III–V are of order $o_P(n^{-1/2})$. Consequently,

$$\sqrt{n}(\tau_\lambda^\lambda \hat{\psi}_1 - \psi_1) = \sqrt{n}(\mathbb{P}_n - \mathbb{E}) \left[\frac{A\{Z - m_1^{\lambda,*}(X)\}}{\pi^*(X)} + m_1^{\lambda,*}(X) \right] + o_P(1). \quad (\text{S2})$$

Similar deviations for the case $a = 0$ lead to

$$\sqrt{n}(\tau_\lambda^\lambda \hat{\psi}_0 - \psi_0) = \sqrt{n}(\mathbb{P}_n - \mathbb{E}) \left[\frac{(1-A)\{Z - m_0^{\lambda,*}(X)\}}{1 - \pi^*(X)} + m_0^{\lambda,*}(X) \right] + o_P(1). \quad (\text{S3})$$

By combining Equations (S2) and (S3), the asymptotic normality of $\tau_\lambda^\lambda \hat{\Delta}_{DR}^\lambda - \Delta^\lambda$ follows from a central limit theorem and Slutsky's lemma, with the fact that $\mathcal{W}_2(\mathcal{I})$ has a bounded diameter (since \mathcal{I} is assumed to be a bounded interval of \mathbb{R}) and thus Z , $m_0^{\lambda,*}(X)$ and $m_1^{\lambda,*}(X)$ have finite variance. \square

Claim 1. $\text{I} = o_P(n^{-1/2})$.

This claim is due to Assumptions 5(b) and 7(b).

Claim 2. $\text{II} = O_P(n^{-1/2})$.

This is a direct consequence of a central limit theorem, with the fact that $\mathcal{W}_2(\mathcal{I})$ has a bounded diameter and thus Z and $m_1^{\lambda,*}(X)$ have finite variance.

Claim 3. $\text{III} = O(\varrho_\pi \varrho_m + n^{-1/2} \varrho_m + n^{-1/2} \varrho_\pi) + O(n^{-1/2} \varrho_m^{1/2})$.

By Cauchy–Schwartz inequality, with Assumption 5(a), we have

$$\begin{aligned}
\text{III} &= \left\| \mathbb{E}_n \left[\frac{\{\tilde{m}_1^\lambda(X) - m_1^\lambda(X)\} \{\hat{\pi}(X) - A\}}{\hat{\pi}(X)} \right] \right\|_\lambda \\
&\leq c \left\| \mathbb{E}_n \left[\{\tilde{m}_1^\lambda(X) - m_1^\lambda(X)\} \{\hat{\pi}(X) - A\} \right] \right\|_\lambda \\
&\leq c \mathbb{E}_n \left\| \{\tilde{m}_1^\lambda(X) - m_1^\lambda(X)\} \{\hat{\pi}(X) - \pi(X)\} \right\|_\lambda + c \left\| \mathbb{E}_n \left[\{\tilde{m}_1^\lambda(X) - m_1^\lambda(X)\} \{\pi(X) - A\} \right] \right\|_\lambda \\
&\leq cn^{-1} \sum_{i=1}^n \sqrt{\mathbb{E} \{ |\hat{\pi}(X_i) - \pi(X_i)|^2 \} \mathbb{E} \{ \|\tilde{m}_1^\lambda(X_i) - m_1^\lambda(X_i)\|_\lambda^2 \}} + O(n^{-1/2} \varrho_m^{1/2}) \\
&= O(\varrho_\pi \varrho_m + n^{-1/2} \varrho_m + n^{-1/2} \varrho_\pi) + O(n^{-1/2} \varrho_m^{1/2}),
\end{aligned}$$

where c is a constant depending on the constant ϵ in Assumption 5(a), and the last equality is obtained by using Assumption 7(a). In the above, the third inequality relies on the bound

$$\left\| \mathbb{E}_n \left[\{\tilde{m}_1^\lambda(X) - m_1^\lambda(X)\} \{\pi(X) - A\} \right] \right\|_\lambda = O(n^{-1/2} \varrho_m^{1/2}), \quad (\text{S4})$$

which we establish below. Let $V_i(g) = \{g(X_i) - m_1^\lambda(X_i)\} \{\pi(X_i) - A\}$, $\eta_i(g, h) = \|g(X_i) - h(X_i)\|_\lambda$, $\eta^2(g, h) = \frac{1}{n} \sum_{i=1}^n \eta_i^2(g, h)$, and $S_n(g) = \frac{1}{\sqrt{n}} \sum_{i=1}^n V_i(g)$. Then $S_n(m_1^\lambda) = 0$, $\mathbb{E}\{V_i(g)\} = 0$ and $\mathbb{E}\{S_n(g)\} = 0$ for all g . In addition, $\|V_i(g) - V_i(h)\|_\lambda \leq |\pi(X_i) - A| \eta_i(g, h) \leq 2\eta_i(g, h)$. Then, according to Assumption 7(c) and Theorem 5, holding \mathbb{X} fixed, we deduce that, for some universal constants $c_0, b_0, r > 0$,

$$\text{pr} \left(\sup_{g \in B_r(m_1^\lambda)} \frac{\|S_n(g)\|_\lambda}{\eta(g, m_1^\lambda)^{1/2}} \geq b\sqrt{K} \mid \mathbb{X} \right) \leq \exp \left(-\frac{c_0 b K}{r} \right)$$

holds for all $b \geq b_0$. This further implies that

$$\mathbb{E} \left(\sup_{g \in B_r(m_1^\lambda)} \frac{\|S_n(g)\|_\lambda}{\eta(g, m_1^\lambda)^{1/2}} \mid \mathbb{X} \right) \leq c_1$$

for a fixed constant c_1 for all \mathbb{X} , and further, $\mathbb{E}(\|S_n(g)\|_\lambda \mid \mathbb{X}) \leq c_1 \eta(g, m_1^\lambda)^{1/2}$ for all $g \in B_r(m_1^\lambda)$. By assumption, $\tilde{m}_1^\lambda \in B_r(m_1^\lambda)$ almost surely, and thus $\mathbb{E}(\|S_n(\tilde{m}_1^\lambda)\|_\lambda \mid \mathbb{X}) \leq c_1 \eta(\tilde{m}_1^\lambda, m_1^\lambda)^{1/2}$. Consequently,

$$\left\| \mathbb{E}_n \left[\{\tilde{m}_1^\lambda(X) - m_1^\lambda(X)\} \{\pi(X) - A\} \right] \right\|_\lambda = n^{-1/2} \mathbb{E} S_n(\tilde{m}_1^\lambda) \leq n^{-1/2} \mathbb{E}(\|S_n(\tilde{m}_1^\lambda)\|_\lambda)$$

$$\begin{aligned} &\leq c_1 n^{-1/2} \mathbb{E} \eta(\tilde{m}_1^\lambda, m_1^\lambda)^{1/2} \leq c_1 n^{-1/2} \{\mathbb{E} \eta^2(\tilde{m}_1^\lambda, m_1^\lambda)\}^{1/4} \\ &= O(n^{-1/2} \varrho_m^{1/2}). \end{aligned}$$

Claim 4. $IV = O_P(n^{-1/2} \varrho_\pi + \varrho_\pi \nu_n + \varrho_\pi \alpha_n + n^{-1}) + o_P(n^{-1/2})$.

We first observe that

$$\mathbb{P}_n \left[\left\{ \frac{A}{\hat{\pi}(X)} - 1 \right\} D_1(X) \right] = \underbrace{\mathbb{P}_n \left[\left\{ \frac{A}{\pi(X)} - 1 \right\} D_1(X) \right]}_{IV_1} + \underbrace{\mathbb{P}_n \left[\left\{ \frac{A\{\pi(X) - \hat{\pi}(X)\}}{\hat{\pi}(X)\pi(X)} \right\} D_1(X) \right]}_{IV_2}.$$

The term IV_1 can be shown to have the order $o_P(n^{-1/2})$ by an argument that is similar to the derivation of (S4). For the second term, we have

$$\begin{aligned} \|\mathbf{IV}_2\|_\lambda &\leq \mathbb{P}_n \|\{\pi(X) - \hat{\pi}(X)\} D_1(X)\|_\lambda \\ &\leq \sqrt{\mathbb{P}_n |\pi(X) - \hat{\pi}(X)|^2 \mathbb{P}_n \|D_1(X)\|_\lambda^2} \\ &= O_P((\varrho_\pi + n^{-1/2})(W_2(\hat{\lambda}, \lambda) + \nu_n + \alpha_n)) \\ &= O_P(n^{-1/2} \varrho_\pi + \varrho_\pi \nu_n + \varrho_\pi \alpha_n + n^{-1}) \end{aligned}$$

where, the first inequality is due to Assumptions 2 and 5(a) on π and $\hat{\pi}$, and the last two equalities are derived by using Assumptions 4 and 6, as well as the assumed rates of ν_n and α_n .

Claim 5. $V = O_P(\alpha_n + \nu_n)$.

We observe that

$$\mathbb{P}_n \left[\frac{AR}{\hat{\pi}(X)} \right] = \mathbb{P}_n \left[\frac{AR}{\pi(X)} \right] + \mathbb{P}_n \left[\frac{AR}{\hat{\pi}(X)} - \frac{AR}{\pi(X)} \right],$$

where the second term is dominated by the first one. Moreover,

$$\mathbb{P}_n \left[\frac{AR}{\pi(X)} \right] = \mathbb{P}_n \left[\frac{AU}{\pi(X)} \right] + \mathbb{P}_n \left[\frac{AV}{\pi(X)} \right], \quad (\text{S5})$$

where $U_i = \tau_{\hat{\lambda}}^\lambda \mathcal{L}_{\hat{\lambda}} Y_i - \mathcal{L}_\lambda Y_i = 0$ and $V_i = \tau_{\hat{\lambda}}^\lambda \mathcal{L}_{\hat{\lambda}} \hat{Y}_i - \tau_{\hat{\lambda}}^\lambda \mathcal{L}_{\hat{\lambda}} Y_i = \mathcal{L}_\lambda \hat{Y}_i - \mathcal{L}_\lambda Y_i$. The claim is then proved by using Lemma 6.

Remark 8. In the paper, \mathcal{I} is assumed to be a bounded interval of \mathbb{R} , which implies that $\mathcal{W}_2(\mathcal{I})$ has a bounded diameter. This boundedness assumption, however, can be dropped if we require

$\mathbb{E}W_2^2(Y, y) < \infty$ for some $y \in \mathcal{W}_2(\mathcal{I})$ and $\|m_a^{\lambda, *}\|_\lambda < \infty$ for $a = 0, 1$, so that Claim 2 remains valid.

5 Proof of Theorem 4

For simplicity, we assume $K = 2$; the general case can be proved in a similar fashion. Let $\mathbb{P}_{n_k} O$ denote $n_k^{-1} \sum_{i \in \mathcal{D}_k} O(A_i, X_i, \hat{Y}_i)$ and $\mathbb{E}_{n_k} O = n_k^{-1} \sum_{i \in \mathcal{D}_k} \mathbb{E}\{O(A_i, X_i, \hat{Y}_i)\}$, where $O = O(A, X, \hat{Y})$ is a random quantity dependent on (A, X, \hat{Y}) . Similarly, we use $\mathbb{P}_n O$ to denote $n^{-1} \sum_{i=1}^n O(A_i, X_i, Y_i)$. As in the previous section, let $Z_i = \mathcal{L}_\lambda Y_i$, where we recall the notation $\mathcal{L}_{\lambda\nu} = \nu^{-1} \circ \lambda$. If the i th subject belongs to the k partition, then $\hat{Z}_i = \mathcal{L}_{\hat{\lambda}_k} \hat{Y}_i$ and $R_i = \tau_{\hat{\lambda}_k}^\lambda \hat{Z}_i - Z_i$, and define $D_{a,k}(x) = \tau_{\hat{\lambda}_k}^\lambda \hat{m}_{a,k}^{\hat{\lambda}_k}(x) - \tilde{m}_{a,k}^\lambda(x)$. The quantity R_i can be viewed as the residual due to the discrepancy between $\hat{\lambda}_k$ and λ , and between \hat{Y}_i and Y_i . Define

$$\begin{aligned}\psi_1 &:= \mathbb{E} \left[\frac{A \mathcal{L}_\lambda Y}{\pi(X)} - \left\{ \frac{A}{\pi(X)} - 1 \right\} m_1^\lambda(X) \right], \\ \psi_0 &:= \mathbb{E} \left[\frac{(1-A) \mathcal{L}_\lambda Y}{1-\pi(X)} - \left\{ \frac{1-A}{1-\pi(X)} - 1 \right\} m_0^\lambda(X) \right]\end{aligned}$$

and their sample versions in each data partition \mathcal{D}_k

$$\begin{aligned}\hat{\psi}_{1,k} &:= \mathbb{P}_{n_{3-k}} \left[\frac{A \mathcal{L}_{\hat{\lambda}_k} \hat{Y}}{\hat{\pi}_k(X)} - \left\{ \frac{A}{\hat{\pi}_k(X)} - 1 \right\} \hat{m}_{1,k}^{\hat{\lambda}_k}(X) \right], \\ \hat{\psi}_{0,k} &:= \mathbb{P}_{n_{3-k}} \left[\frac{(1-A) \mathcal{L}_{\hat{\lambda}_k} \hat{Y}}{1-\hat{\pi}_k(X)} - \left\{ \frac{1-A}{1-\hat{\pi}_k(X)} - 1 \right\} \hat{m}_{0,k}^{\hat{\lambda}_k}(X) \right].\end{aligned}$$

Then we have $\Delta^\lambda = \psi_1 - \psi_0$ and $\hat{\Delta}_{DR}^{\hat{\lambda}} = n^{-1}(n_1 \tau_{\hat{\lambda}_1}^{\hat{\lambda}} \hat{\psi}_{1,1} + n_2 \tau_{\hat{\lambda}_2}^{\hat{\lambda}} \hat{\psi}_{1,2}) - n^{-1}(n_1 \tau_{\hat{\lambda}_1}^{\hat{\lambda}} \hat{\psi}_{0,1} + n_2 \tau_{\hat{\lambda}_2}^{\hat{\lambda}} \hat{\psi}_{0,2})$ for the cross-fitting estimator defined in (9), and consequently,

$$\tau_{\hat{\lambda}}^{\hat{\lambda}} \hat{\Delta}_{DR}^{\hat{\lambda}} = n^{-1}(n_1 \tau_{\hat{\lambda}_1}^\lambda \hat{\psi}_{1,1} + n_2 \tau_{\hat{\lambda}_2}^\lambda \hat{\psi}_{1,2}) - n^{-1}(n_1 \tau_{\hat{\lambda}_1}^\lambda \hat{\psi}_{0,1} + n_2 \tau_{\hat{\lambda}_2}^\lambda \hat{\psi}_{0,2}).$$

In the above, when $\hat{\lambda}_k = \lambda$, the operator $\tau_{\hat{\lambda}_k}^\lambda$ is an identity operator and has no effect. The proof will be based on the following decomposition for $n^{-1}(n_1 \tau_{\hat{\lambda}_1}^\lambda \hat{\psi}_{1,1} + n_2 \tau_{\hat{\lambda}_2}^\lambda \hat{\psi}_{1,2})$:

$$\begin{aligned}& n^{-1}(n_1 \tau_{\hat{\lambda}_1}^\lambda \hat{\psi}_{1,1} + n_2 \tau_{\hat{\lambda}_2}^\lambda \hat{\psi}_{1,2}) - \psi_1 \\ &= n^{-1} \sum_{k=1,2} n_{3-k} \mathbb{P}_{n_{3-k}} \left[\frac{AZ + AR}{\hat{\pi}_k(X)} - \left\{ \frac{A}{\hat{\pi}_k(X)} - 1 \right\} \{\tilde{m}_{1,k}^\lambda(X) + D_{1,k}(X)\} \right] - \psi_1\end{aligned}$$

$$\begin{aligned}
&= n^{-1} \sum_{k=1,2} n_{3-k} (\mathbb{P}_{n_{3-k}} - \mathbb{E}_{n_{3-k}}) \underbrace{\left[\frac{A\{Z - \tilde{m}_{1,k}^\lambda(X)\}}{\hat{\pi}_k(X)} + \tilde{m}_{1,k}^\lambda(X) - \frac{A\{Z - m_1^{\lambda,*}(X)\}}{\pi^*(X)} - m_1^{\lambda,*}(X) \right]}_{\text{I}} \\
&+ n^{-1} \sum_{k=1,2} n_{3-k} (\mathbb{P}_{n_{3-k}} - \mathbb{E}_{n_{3-k}}) \underbrace{\left[\frac{A\{Z - m_1^{\lambda,*}(X)\}}{\pi^*(X)} + m_1^{\lambda,*}(X) \right]}_{\text{II}} \\
&+ n^{-1} \sum_{k=1,2} n_{3-k} \mathbb{E}_{n_{3-k}} \underbrace{\left[\frac{\{\tilde{m}_{1,k}^\lambda(X) - m_1^\lambda(X)\} \{\hat{\pi}_k(X) - A\}}{\hat{\pi}_k(X)} \right]}_{\text{III}} \\
&+ n^{-1} \sum_{k=1,2} n_{3-k} \mathbb{P}_{n_{3-k}} \underbrace{\left[\left\{ 1 - \frac{A}{\hat{\pi}_k(X)} \right\} D_{1,k}(X) \right]}_{\text{IV}} \\
&+ n^{-1} \sum_{k=1,2} n_{3-k} \mathbb{P}_{n_{3-k}} \underbrace{\left\{ \frac{AR}{\hat{\pi}_k(X)} \right\}}_{\text{V}}.
\end{aligned}$$

The decomposition for the other term is similar and thus omitted.

The symbol \mathcal{D}_k below is used to denote both the data in the k th partition (when it appears in a conditional expectation or probability) and their indices (when it appears in the subscript of a summation). Let $b_m = \max\{\|m_a^\lambda - m_a^{\lambda,*}\| : a = 0, 1\}$ and $b_\pi = \|\pi - \pi^*\|_2$. Note that $b_\pi = 0$ when $\varrho_\pi = o_P(1)$ and $b_m = 0$ when $\varrho_m = o(1)$, as in these cases, $\pi = \pi^*$ and $m_a^\lambda = m_a^{\lambda,*}$.

Proof of part (i). This is a direct consequence of Claims 6–10, given that $b_\pi = O(1)$, $b_m = O(1)$, $\nu_n = o(n^{-1/2})$ and $\alpha_n = o(n^{-1/2})$. \square

Proof of part (ii). Under the assumed conditions, $b_m = b_\pi = 0$ and the terms I and III–V are of order $o_P(n^{-1/2})$. Consequently,

$$\sqrt{n}(n^{-1}(n_1\tau_{\hat{\lambda}_1}^\lambda \hat{\psi}_{1,1} + n_2\tau_{\hat{\lambda}_2}^\lambda \hat{\psi}_{1,2}) - \psi_1) = \sqrt{n}(\mathbb{P}_n - \mathbb{E}) \left[\frac{A\{Z - m_1^{\lambda,*}(X)\}}{\pi^*(X)} + m_1^{\lambda,*}(X) \right] + o_P(1). \tag{S6}$$

Similar deviations for the case $a = 0$ lead to

$$\sqrt{n}(n^{-1}(n_1\tau_{\hat{\lambda}_0}^\lambda \hat{\psi}_{0,1} + n_2\tau_{\hat{\lambda}_2}^\lambda \hat{\psi}_{0,2}) - \psi_0) = \sqrt{n}(\mathbb{P}_n - \mathbb{E}) \left[\frac{(1-A)\{Z - m_0^{\lambda,*}(X)\}}{1 - \pi^*(X)} + m_0^{\lambda,*}(X) \right] + o_P(1). \tag{S7}$$

By combining (S6) and (S7), the asymptotic normality of $\tau_{\hat{\lambda}}^\lambda \hat{\Delta}_{DR}^\lambda - \Delta^\lambda$ follows from a central limit theorem and Slutsky's lemma, with the fact that $\mathcal{W}_2(\mathcal{I})$ has a bounded diameter (since

\mathcal{I} is assumed to be a bounded interval of \mathbb{R} and thus Z , $m_0^{\lambda,*}(X)$ and $m_1^{\lambda,*}(X)$ have finite variance. \square

Claim 6. $\mathbf{I} = O_P(n^{-1/2}\varrho_\pi + n^{-1/2}\varrho_m + \varrho_\pi\varrho_m + n^{-1/2}b_\pi + n^{-1/2}b_m)$.

To prove the claim, let

$$\begin{aligned} G(A, X, Z) &= \frac{A\{Z - \tilde{m}_{1,k}^\lambda(X)\}}{\hat{\pi}_k(X)} + \tilde{m}_{1,k}^\lambda(X) - m_1^\lambda(X), \\ H_1(A, X, Z) &= \frac{AZ\{\pi^*(X) - \hat{\pi}_k(X)\}}{\hat{\pi}_k(X)\pi^*(X)}, \\ H_2(A, X, Z) &= \frac{A\{\hat{\pi}_k(X)m_1^{\lambda,*}(X) - \pi^*(X)\tilde{m}_{1,k}^\lambda(X)\}}{\hat{\pi}_k(X)\pi^*(X)}, \\ H_3(A, X, Z) &= \tilde{m}_{1,k}^\lambda(X) - m_1^{\lambda,*}(X), \\ H(A, X, Z) &= H_1(A, X, Z) + H_2(A, X, Z) + H_3(A, X, Z). \end{aligned}$$

Then

$$\begin{aligned} \mathbb{E}(\|\mathbf{I}\|_\lambda^2) &= \frac{1}{n_{3-k}^2} \sum_{i \in \mathcal{D}_{3-k}} \mathbb{E}\|H(A_i, X_i, Z_i) - \mathbb{E}H(A_i, X_i, Z_i)\|_\lambda^2 \\ &\quad + \frac{1}{n_{3-k}^2} \sum_{\substack{i, j \in \mathcal{D}_{3-k} \\ i \neq j}} \mathbb{E}\langle H(A_i, X_i, Z_i) - \mathbb{E}H(A_i, X_i, Z_i), H(A_j, X_j, Z_j) - \mathbb{E}H(A_j, X_j, Z_j) \rangle_\lambda \\ &\equiv \mathbf{I}_1 + \mathbf{I}_2. \end{aligned}$$

For the first term \mathbf{I}_1 , we further have

$$\begin{aligned} \mathbf{I}_1 &\leq \frac{1}{n_{3-k}^2} \sum_{i \in \mathcal{D}_{3-k}} \mathbb{E}\|H(A_i, X_i, Z_i)\|_\lambda^2 \\ &\leq \frac{1}{n_{3-k}^2} \sum_{i \in \mathcal{D}_{3-k}} \{\mathbb{E}\|H_1(A_i, X_i, Z_i)\|_\lambda^2 + \mathbb{E}\|H_2(A_i, X_i, Z_i)\|_\lambda^2 + \mathbb{E}\|H_3(A_i, X_i, Z_i)\|_\lambda^2\}. \end{aligned}$$

By Assumption 5(a) and the fact that $\mathcal{W}_2(\mathcal{I})$ is bounded, for (A, X, Z) whose index is in D_{3-k} , we deduce that

$$\begin{aligned} \mathbb{E}\|H_2(A, X, Z)\|_\lambda^2 &\leq c\mathbb{E}\|\hat{\pi}_k(X)m_1^{\lambda,*}(X) - \pi^*(X)\tilde{m}_{1,k}^\lambda(X)\|_\lambda^2 \\ &\leq c\mathbb{E}\|\hat{\pi}_k(X)m_1^{\lambda,*}(X) - \pi(X)m_1^{\lambda,*}(X)\|_\lambda^2 \\ &\quad + c\mathbb{E}\|\pi(X)m_1^{\lambda,*}(X) - \pi(X)\tilde{m}_{1,k}^\lambda(X)\|_\lambda^2 \\ &\quad + c\mathbb{E}\|\pi(X)\tilde{m}_{1,k}^\lambda(X) - \pi^*(X)\tilde{m}_{1,k}^\lambda(X)\|_\lambda^2 \end{aligned}$$

$$\begin{aligned}
&\leq c\mathbb{E}|\hat{\pi}_k(X) - \pi(X)|^2 + c\mathbb{E}\|m_1^{\lambda,*}(X) - \tilde{m}_{1,k}^\lambda(X)\|_\lambda^2 + c\mathbb{E}|\pi(X) - \pi^*(X)|^2 \\
&\leq c\mathbb{E}\|\hat{\pi}_k - \pi\|_2^2 + c\mathbb{E}\|m_1^{\lambda,*} - \tilde{m}_{1,k}^\lambda\|_\lambda^2 + c\|\pi - \pi^*\|_2^2 \\
&\leq c\varrho_\pi^2 + c\varrho_m^2 + cb_\pi^2.
\end{aligned}$$

Similarly, we have $\mathbb{E}\|H_1(A, X, Z)\|_\lambda^2 \leq cb_\pi^2 + c\varrho_\pi^2$ and $\mathbb{E}\|H_3(A, X, Z)\|_\lambda^2 \leq c\varrho_m^2 + cb_m^2$. These imply that $\mathbb{E}\|H(A_i, X_i, Z_i)\|_\lambda^2 \leq c\varrho_\pi^2 + c\varrho_m^2 + cb_\pi^2 + cb_m^2$ and further

$$\mathbf{I}_1 = O(n^{-1}(\varrho_\pi^2 + \varrho_m^2 + b_\pi^2 + b_m^2)).$$

For the term \mathbf{I}_2 , simple calculation shows that

$$\mathbb{E}\{G(A_i, X_i, Z_i) \mid \mathcal{D}_k, X_i\} = \frac{\{\pi(X_i) - \hat{\pi}_k(X_i)\}\{m_1^\lambda(X_i) - \tilde{m}_{1,k}^\lambda(X_i)\}}{\hat{\pi}_k(X_i)}$$

and consequently

$$\mathbb{E}[\|\mathbb{E}\{G(A_i, X_i, Z_i) \mid \mathcal{D}_k, X_i\}\|_\lambda \mid \mathcal{D}_k] \leq c\|\pi - \hat{\pi}_k\|_2\|m_1^\lambda - \tilde{m}_{1,k}^\lambda\|_\lambda$$

and

$$\|\mathbb{E}G(A_i, X_i, Z_i)\|_\lambda \leq c\mathbb{E}\{|\pi(X_i) - \hat{\pi}_k(X_i)|\|m_1^\lambda(X_i) - \tilde{m}_{1,k}^\lambda(X_i)\|_\lambda\} \leq c\varrho_\pi\varrho_m.$$

where we utilize Assumption 5(a). Therefore, we deduce that

$$\begin{aligned}
&|\mathbb{E}\langle H(A_i, X_i, Z_i) - \mathbb{E}H(A_i, X_i, Z_i), H(A_j, X_j, Z_j) - \mathbb{E}H(A_j, X_j, Z_j) \rangle_\lambda| \\
&|\mathbb{E}\langle G(A_i, X_i, Z_i) - \mathbb{E}G(A_i, X_i, Z_i), G(A_j, X_j, Z_j) - \mathbb{E}G(A_j, X_j, Z_j) \rangle_\lambda| \\
&= |\mathbb{E}\langle G(A_i, X_i, Z_i), G(A_j, X_j, Z_j) \rangle_\lambda - \langle \mathbb{E}G(A_i, X_i, Z_i), \mathbb{E}G(A_j, X_j, Z_j) \rangle_\lambda| \\
&\leq |\mathbb{E}\mathbb{E}\{\langle G(A_i, X_i, Z_i), G(A_j, X_j, Z_j) \rangle_\lambda \mid \mathcal{D}_k\}| + \|\mathbb{E}G(A_i, X_i, Z_i)\|_\lambda\|\mathbb{E}G(A_j, X_j, Z_j)\|_\lambda \\
&\leq \mathbb{E}\|\mathbb{E}\{G(A_i, X_i, Z_i) \mid \mathcal{D}_k\}\|_\lambda\|\mathbb{E}\{G(A_j, X_j, Z_j) \mid \mathcal{D}_k\}\|_\lambda + c\varrho_\pi^2\varrho_m^2 \\
&\leq c\mathbb{E}\{\|\pi - \hat{\pi}_k\|_2^2\|m_1^\lambda - \tilde{m}_{1,k}^\lambda\|_\lambda^2\} + c\varrho_\pi^2\varrho_m^2 \\
&\leq c\varrho_\pi^2\varrho_m^2.
\end{aligned}$$

This result, together with Assumption 9, implies that $\mathbf{I}_2 = O(\varrho_\pi^2\varrho_m^2)$. Combining this with the order for \mathbf{I}_1 , we show that

$$\mathbb{E}(\|\mathbf{I}\|_\lambda^2) = O(n^{-1}\varrho_\pi^2 + n^{-1}\varrho_m^2 + \varrho_\pi^2\varrho_m^2 + n^{-1}b_\pi^2 + n^{-1}b_m^2), \quad (\text{S8})$$

which implies Claim 6.

Claim 7. $\text{II} = O_P(n^{-1/2})$.

This is a direct consequence of a central limit theorem, with the fact that $\mathcal{W}_2(\mathcal{I})$ has a bounded diameter and thus both Z and $m_1^{\lambda,*}(X)$ have finite variance.

Claim 8. $\text{III} = O(\varrho_\pi \varrho_m)$.

By Cauchy–Schwartz inequality, with Assumption 5(a), we have

$$\begin{aligned}
\|\text{III}\|_\lambda &= \left\| \mathbb{E}_{n_{3-k}} \mathbb{E} \left[\frac{\{\tilde{m}_{1,k}^\lambda(X) - m_1^\lambda(X)\} \{\hat{\pi}_k(X) - A\}}{\hat{\pi}_k(X)} \middle| \mathcal{D}_k \right] \right\|_\lambda \\
&= \left\| \mathbb{E}_{n_{3-k}} \left[\frac{\{\tilde{m}_{1,k}^\lambda(X) - m_1^\lambda(X)\} \{\hat{\pi}_k(X) - \pi(X)\}}{\hat{\pi}_k(X)} \right] \right\|_\lambda \\
&\leq c \left\| \mathbb{E}_{n_{3-k}} \left[\{\tilde{m}_{1,k}^\lambda(X) - m_1^\lambda(X)\} \{\hat{\pi}_k(X) - \pi(X)\} \right] \right\|_\lambda \\
&\leq c \mathbb{E}_{n_{3-k}} \left\| \{\tilde{m}_{1,k}^\lambda(X) - m_1^\lambda(X)\} \{\hat{\pi}_k(X) - \pi(X)\} \right\|_\lambda \\
&= O(\varrho_\pi \varrho_m). \tag{S9}
\end{aligned}$$

Claim 9. $\text{IV} = O_P(n^{-1} + n^{-1/2} \nu_n + n^{-1/2} \alpha_n + n^{-1/2} \varrho_\pi + \varrho_\pi \nu_n + \varrho_\pi \alpha_n)$.

Consider

$$\begin{aligned}
\|\text{IV}\|_\lambda^2 &= \underbrace{n_{3-k}^{-2} \sum_{i \in \mathcal{D}_k} \left\| \left\{ 1 - \frac{A_i}{\hat{\pi}_k(X_i)} \right\} D_{1,k}(X_i) \right\|_\lambda^2}_{\text{IV}_1} \\
&\quad + \underbrace{n_{3-k}^{-2} \sum_{\substack{i,j \in \mathcal{D}_k \\ i \neq j}} \left\langle \left\{ 1 - \frac{A_i}{\hat{\pi}_k(X_i)} \right\} D_{1,k}(X_i), \left\{ 1 - \frac{A_j}{\hat{\pi}_k(X_j)} \right\} D_{1,k}(X_j) \right\rangle_\lambda}_{\text{IV}_2}.
\end{aligned}$$

It is seen that $\text{IV}_1 \leq cn_{3-k}^{-2} \sum_{i \in \mathcal{D}_k} \|D_{1,k}(X_i)\|_\lambda^2$, where Assumption 5(a) is utilized. For any $\delta > 0$,

$$\begin{aligned}
&\text{pr} \left(n_{3-k}^{-1} \sum_{i \in \mathcal{D}_k} \|D_{1,k}(X_i)\|_\lambda^2 \leq \delta^{-1} \left\| \tau_{\hat{\lambda}_k}^\lambda \hat{m}_{1,k}^{\hat{\lambda}_k} - \tilde{m}_{1,k}^\lambda \right\|_\lambda^2 \middle| \mathcal{D}_k \right) \\
&\leq \delta \frac{n_{3-k}^{-1} \sum_{i \in \mathcal{D}_k} \mathbb{E} \{ \|D_{1,k}(X_i)\|_\lambda^2 \mid \mathcal{D}_k \}}{\left\| \tau_{\hat{\lambda}_k}^\lambda \hat{m}_{1,k}^{\hat{\lambda}_k} - \tilde{m}_{1,k}^\lambda \right\|_\lambda^2} \\
&= \delta,
\end{aligned}$$

which then implies that $\text{pr}\left(n_{3-k}^{-1} \sum_{i \in \mathcal{D}_k} \|D_{1,k}(X_i)\|_\lambda^2 \leq \delta^{-1} \left\| \tau_{\hat{\lambda}_k}^\lambda \hat{m}_{1,k}^{\hat{\lambda}_k} - \tilde{m}_{1,k}^\lambda \right\|_\lambda^2\right) \leq \delta$ for arbitrary $\delta > 0$, or equivalently, $n_{3-k}^{-1} \sum_{i \in \mathcal{D}_k} \|D_{1,k}(X_i)\|_\lambda^2 \leq \delta^{-1} \left\| \tau_{\hat{\lambda}_k}^\lambda \hat{m}_{1,k}^{\hat{\lambda}_k} - \tilde{m}_{1,k}^\lambda \right\|_\lambda^2 = O_P\left(\left\| \tau_{\hat{\lambda}_k}^\lambda \hat{m}_{1,k}^{\hat{\lambda}_k} - \tilde{m}_{1,k}^\lambda \right\|_\lambda^2\right)$. With Assumptions 4, 8 and 9, we conclude that $\|\text{IV}_1\|_\lambda^2 = O_P(n^{-2} + n^{-1}\nu_n^2 + n^{-1}\alpha_n^2)$. Similarly, we can deduce that $\|\text{IV}_2\|_\lambda^2 = O_P(\|\hat{\pi}_k - \pi\|_2^2 \|D_{1,k}\|_\lambda^2) = O_P(n^{-1}\varrho_\pi^2 + \varrho_\pi^2 \nu_n^2 + \varrho_\pi^2 \alpha_n^2)$. Consequently, we obtain

$$\text{IV} = O_P(n^{-1} + n^{-1/2}\nu_n + n^{-1/2}\alpha_n + n^{-1/2}\varrho_\pi + \varrho_\pi \nu_n + \varrho_\pi \alpha_n). \quad (\text{S10})$$

Claim 10. $V = O_P(\alpha_n + \nu_n)$.

For a proof, we observe that

$$\mathbb{P}_{n_{3-k}} \left[\frac{AR}{\hat{\pi}_k(X)} \right] = \mathbb{P}_{n_{3-k}} \left[\frac{AR}{\pi(X)} \right] + \mathbb{P}_n \left[\frac{AR}{\hat{\pi}_k(X)} - \frac{AR}{\pi(X)} \right],$$

where the second term is dominated by the first one. Moreover,

$$\mathbb{P}_{n_{3-k}} \left[\frac{AR}{\pi(X)} \right] = \mathbb{P}_{n_{3-k}} \left[\frac{AU}{\pi(X)} \right] + \mathbb{P}_{n_{3-k}} \left[\frac{AV}{\pi(X)} \right],$$

where $U = \tau_{\hat{\lambda}_k}^\lambda \mathcal{L}_{\hat{\lambda}_k} Y - \mathcal{L}_\lambda Y = 0$ and $V = \tau_{\hat{\lambda}_k}^\lambda \mathcal{L}_{\hat{\lambda}_k} \hat{Y} - \tau_{\hat{\lambda}_k}^\lambda \mathcal{L}_{\hat{\lambda}_k} Y = \mathcal{L}_\lambda \hat{Y} - \mathcal{L}_\lambda Y$. By Lemma 6 and the assumptions on α_n and ν_n , we deduce that

$$V = O_P(\alpha_n + \nu_n). \quad (\text{S11})$$

Remark 9. As in Remark 8, when the assumption on boundedness of \mathcal{I} is dropped, for Claim 7 to hold, we require the second moment condition that $\mathbb{E}W_2^2(Y, y) < \infty$ for some $y \in \mathcal{W}_2(\mathcal{I})$ and $\|m_a^{\lambda,*}\|_\lambda < \infty$. In addition, Claim 6 requires the additional condition that $\mathbb{E}\|\tilde{m}_{a,k}^\lambda\|_\lambda^2 < \infty$ and $\|m_a^{\lambda,*}\|_\lambda < \infty$, for $a = 0, 1$ and all k . This is because, under the new condition, we bound the term

$$\begin{aligned} \mathbb{E}\|\pi(X)\tilde{m}_{1,k}^\lambda(X) - \pi^*(X)\tilde{m}_{1,k}^\lambda(X)\|_\lambda^2 &= \mathbb{E}\mathbb{E}\{\|\pi(X)\tilde{m}_{1,k}^\lambda(X) - \pi^*(X)\tilde{m}_{1,k}^\lambda(X)\|_\lambda^2 \mid \mathcal{D}_k\} \\ &= \mathbb{E}\{\|\pi - \pi^*\|_2^2 \|\tilde{m}_{1,k}^\lambda\|_\lambda^2\} \\ &\leq \|\pi - \pi^*\|_2^2 \mathbb{E}\|\tilde{m}_{1,k}^\lambda\|_\lambda^2 = O(b_\pi^2) \end{aligned}$$

when we derive the order for $\mathbb{E}\|H_2(A, X, Z)\|_\lambda^2$ and X is not in \mathcal{D}_k . A similar argument applies to $\mathbb{E}\|\hat{\pi}_k(X)m_1^{\lambda,*}(X) - \pi(X)m_1^{\lambda,*}(X)\|_\lambda^2$ and $\mathbb{E}\|H_1(A, X, Z)\|_\lambda^2$.

6 Technical Lemmas

Lemma 1. For $G_1, G_2 \in \mathcal{W}_2(\mathcal{I})$ and a probability distribution λ , we have $\|\mathcal{L}_\lambda G_1 - \mathcal{L}_\lambda G_2\|_\lambda = W_2(G_1, G_2)$.

Proof of Lemma 1. The claims follows from the following observations: $\|\mathcal{L}_\lambda G_1 - \mathcal{L}_\lambda G_2\|_\lambda^2 = \int |G_1^{-1} \circ \lambda - G_2^{-1} \circ \lambda|^2 d\lambda = \int_0^1 |G_1^{-1}(t) - G_2^{-1}(t)|^2 dt = W_2^2(G_1, G_2)$, where the last equality is due to Theorem 2.18 of Villani (2003). \square

Lemma 2. For a random element W on $\mathcal{W}_2(\mathcal{I})$, $\mathbb{E}W^{-1} = (\mathbb{E}W)^{-1}$ and $\mathbb{E}\mathcal{L}_\lambda W = \mathcal{L}_\lambda \mathbb{E}W$ for any probability distribution λ .

Proof of Lemma 2. The first assertion is a direct consequence of the isometry between $\mathcal{W}_2(\mathcal{I})$ and the collection of quantile functions, viewed as a subspace of space $L^2(\mathcal{I})$ of squared integrable functions endowed with the L^2 distance $\|f - g\| := \sqrt{\int_{\mathcal{I}} |f(x) - g(x)|_2^2 dx}$ (Theorem 2.18, Villani, 2003).

For the second assertion, $\mathbb{E}\mathcal{L}_\lambda W = \mathbb{E}(W^{-1} \circ \lambda) = (\mathbb{E}W^{-1}) \circ \lambda = (\mathbb{E}W)^{-1} \circ \lambda = \mathcal{L}_\lambda \mathbb{E}W$, where the third equality is due to the first assertion. \square

Lemma 3. For the Fréchet function $F(\cdot) = \mathbb{E}W_2^2(y, Y)$ of a random element Y on a Wasserstein space $\mathcal{W}_2(\mathcal{I})$, we have $F(y) - F(\mu) = W_2^2(y, \mu)$ for all $y \in \mathcal{W}_2(\mathcal{I})$, where μ is the Fréchet mean of Y .

Proof of Lemma 3. Let $\langle g, h \rangle = \int_{\mathcal{I}} g(t)h(t)dt$ for two functions g and h . We first observe that

$$\begin{aligned} F(y) - F(\mu) &= \mathbb{E}W_2^2(y, Y) - \mathbb{E}d^2(\mu, Y) \\ &= \mathbb{E}(\langle y^{-1} - Y^{-1}, y^{-1} - Y^{-1} \rangle - \langle \mu^{-1} - Y^{-1}, \mu^{-1} - Y^{-1} \rangle) \\ &= \langle y^{-1} - \mu^{-1}, y^{-1} - \mu^{-1} \rangle - 2\mathbb{E}\langle y^{-1} - \mu^{-1}, \mu^{-1} - Y^{-1} \rangle \\ &= W_2^2(y, \mu) - 2\langle y^{-1} - \mu^{-1}, \mu^{-1} - \mathbb{E}Y^{-1} \rangle \\ &= W_2^2(y, \mu) \end{aligned}$$

where the second equality is due to the isometry between $\mathcal{W}_2(\mathcal{I})$ and the collection of quantile functions (Theorem 2.18, Villani, 2003), and the last equality is due to $\mathbb{E}Y^{-1} = \mu^{-1}$ shown in Lemma 2. \square

Lemma 4. Suppose that $\hat{\mu}$ is the empirical Fréchet mean of $\hat{Y}_1, \dots, \hat{Y}_n$, and $\tilde{\mu}$ is the empirical Fréchet mean of Y_1, \dots, Y_n residing on \mathcal{M} . Then we have $W_2^2(\tilde{\mu}, \mu) = o_P(1)$, and under additional Assumption 3 we have $W_2^2(\hat{\mu}, \mu) = o_P(1)$.

Proof of Lemma 4. As in the proof of Lemma 3, according to the isometry between $\mathcal{W}_2(\mathcal{I})$ and the collection of quantile functions (Theorem 2.18, Villani, 2003), $W_2^2(\tilde{\mu}, \mu) = o_P(1)$ if and only if $\|\tilde{\mu}^{-1} - \mu^{-1}\|_2^2 = o_P(1)$, where $\|g\|_2^2 = \int_{\mathcal{I}} |g(t)|^2 dt$ for any measurable function g . By Lemma 2, $\tilde{\mu}^{-1} = n^{-1} \sum_{i=1}^n Y_i^{-1}$ and $\mathbb{E}Y_i^{-1} = \mu^{-1}$. Then $\|\tilde{\mu}^{-1} - \mu^{-1}\|_2^2 = o_P(1)$ follows from the weak law of large numbers.

To prove $W_2^2(\hat{\mu}, \mu) = o_P(1)$, we apply Lemma 2 to the uniform distribution on the discrete set $\{\hat{Y}_1, \dots, \hat{Y}_n\}$ and its Fréchet mean $\hat{\mu}$, and deduce $\hat{\mu}^{-1} = (n^{-1} \sum_{i=1}^n \hat{Y}_i^{-1})$. Similarly, $\tilde{\mu}^{-1} = (n^{-1} \sum_{i=1}^n Y_i^{-1})$. Then

$$\begin{aligned} W_2(\hat{\mu}, \tilde{\mu}) &= \|\hat{\mu}^{-1} - \tilde{\mu}^{-1}\|_2 = \left\| n^{-1} \sum_{i=1}^n \hat{Y}_i^{-1} - n^{-1} \sum_{i=1}^n Y_i^{-1} \right\|_2 \\ &\leq n^{-1} \sum_{i=1}^n \|\hat{Y}_i^{-1} - Y_i^{-1}\|_2 = n^{-1} \sum_{i=1}^n W_2(\hat{Y}_i, Y_i) = O_P(\alpha_n) = o_P(1), \end{aligned}$$

where the third equality is due to Assumption 3 and Markov's inequality. Then $W_2(\hat{\mu}, \mu) \leq W_2(\hat{\mu}, \tilde{\mu}) + W_2(\tilde{\mu}, \mu) = o_P(1)$. \square

Lemma 5. *If $\hat{\lambda}$ is continuous, then under Assumption 3,*

$$\frac{1}{n} \sum_{i=1}^n \|\tau_{\hat{\lambda}}^{\lambda} \mathcal{L}_{\hat{\lambda}} \hat{Y}_i - \mathcal{L}_{\lambda} Y_i\|_{\lambda}^2 = O_P(\alpha_n^2 + \nu_n^2).$$

Proof of Lemma 5. Given the following observation

$$\frac{1}{n} \sum_{i=1}^n \|\tau_{\hat{\lambda}}^{\lambda} \mathcal{L}_{\hat{\lambda}} \hat{Y}_i - \mathcal{L}_{\lambda} Y_i\|_{\lambda}^2 \leq \frac{2}{n} \sum_{i=1}^n \|\tau_{\hat{\lambda}}^{\lambda} \mathcal{L}_{\hat{\lambda}} \hat{Y}_i - \mathcal{L}_{\lambda} Y_i\|_{\lambda}^2 + \frac{2}{n} \sum_{i=1}^n \|\tau_{\hat{\lambda}}^{\lambda} \mathcal{L}_{\hat{\lambda}} \hat{Y}_i - \tau_{\hat{\lambda}}^{\lambda} \mathcal{L}_{\hat{\lambda}} Y_i\|_{\lambda}^2,$$

the conclusion is a direct consequence of Lemma 6 and the fact that $\tau_{\hat{\lambda}}^{\lambda} \mathcal{L}_{\hat{\lambda}} Y_i - \mathcal{L}_{\lambda} Y_i = 0$ when $\hat{\lambda}$ is continuous (so that $\hat{\lambda} \circ \hat{\lambda}^{-1} = \text{id}$). \square

Lemma 6. *Under Assumption 3, for a fixed $\epsilon > 0$, we have*

$$\sup_{\lambda} \frac{1}{n} \sum_{i=1}^n \|\mathcal{L}_{\lambda} \hat{Y}_i - \mathcal{L}_{\lambda} Y_i\|_{\lambda}^2 = O_P(\alpha_n^2 + \nu_n^2).$$

Proof of Lemma 6. This directly follows from Lemma 1 and Assumption 3. \square

Lemma 7. *Suppose that $\hat{\mu}$ is the empirical Fréchet mean of $\hat{Y}_1, \dots, \hat{Y}_n \in \mathcal{W}_2(\mathcal{I})$, and $\tilde{\mu}$ is the empirical Fréchet mean of $Y_1, \dots, Y_n \in \mathcal{W}_2(\mathcal{I})$. Then, we have $W_2^2(\tilde{\mu}, \mu) = O_P(n^{-1})$.*

Suppose further that Assumption 3 holds, then we have $W_2^2(\hat{\mu}, \tilde{\mu}) = O_P(\alpha_n^2)$ and $W_2^2(\hat{\mu}, \mu) = O_P(n^{-1} + \alpha_n^2)$.

Proof of Lemma 7. We apply the general theory from Schötz (2019). According to the discussion in Section 3 of Schötz (2019), the weak quadruple condition holds for a Wasserstein space $\mathcal{W}_2(\mathcal{I})$. The moment condition is met given the boundedness of $\mathcal{W}_2(\mathcal{I})$, while the growth condition is verified in Lemma 3. In light of Lemma 4 and according to Schötz (2019), it is sufficient to verify the entropy condition in a neighborhood of μ . Such entropy condition holds as $\sup_{\omega \in \mathcal{W}_2(\mathcal{I})} \log N(\delta\epsilon, B_\delta(\omega), d) \leq K\epsilon^{-1}$ shown in the proof of Proposition 1 of Petersen and Müller (2019).

Now we modify the proof for Theorem 1 of Schötz (2019) to the case that only noisy surrogates $\widehat{Y}_1, \dots, \widehat{Y}_n$ are observable. Let $\tilde{F}_n(y) = n^{-1} \sum_{i=1}^n W_2^2(y, Y_i)$ and $F_n(y) = n^{-1} \sum_{i=1}^n W_2^2(y, \widehat{Y}_i)$. Define

$$\begin{aligned}\tilde{\Xi}_n(\delta) &:= \sup_{y \in \mathcal{M}: W_2(y, \mu) < \delta} \tilde{F}(y) - \tilde{F}(\mu) - \tilde{F}_n(y) + \tilde{F}_n(\mu), \\ \Xi_n(\delta) &:= \sup_{y \in \mathcal{M}: W_2(y, \mu) < \delta} \tilde{F}(y) - \tilde{F}(\mu) - F_n(y) + F_n(\mu).\end{aligned}$$

According to Lemma 2 of Schötz (2019), we just need to show that $\mathbb{E}\{\Xi_n^2(\delta)\} \leq c_1(n^{-1} + \alpha_n^2)\delta^2$ for some constant $c_1 > 0$ and all $\delta > 0$. First, we observe that $\Xi_n(\delta) \leq \tilde{\Xi}_n(\delta) + G_n(\delta)$, where

$$\begin{aligned}G_n(\delta) &= \sup_{y \in \mathcal{M}: W_2(y, \mu) < \delta} \frac{1}{n} \sum_{i=1}^n \{W_2^2(y, \widehat{Y}_i) - W_2^2(y, Y_i) - W_2^2(\mu, \widehat{Y}_i) + W_2^2(\mu, Y_i)\} \\ &\leq \sup_{y \in \mathcal{M}: W_2(y, \mu) < \delta} \frac{1}{n} \sum_{i=1}^n W_2(y, \mu) d(Y_i, \widehat{Y}_i) \leq \frac{\delta}{n} \sum_{i=1}^n W_2(Y_i, \widehat{Y}_i),\end{aligned}$$

where the first inequality is due to the Weak Quadruple condition; see Section 3.2.3 of Schötz (2019) for details. Thus, according to Assumption 3,

$$\mathbb{E}\{G_n^2(\delta)\} \leq \delta^2 \mathbb{E} \left\{ \frac{1}{n} \sum_{i=1}^n W_2(Y_i, \widehat{Y}_i) \right\}^2 \leq \frac{\delta^2}{n} \sum_{i=1}^n \mathbb{E} W_2^2(Y_i, \widehat{Y}_i) \leq \delta^2 \alpha_n^2.$$

According to Lemma 3 of Schötz (2019), we have $\mathbb{E}\{\tilde{\Xi}_n^2(\delta)\} \leq c_2\delta^2/n$ for some constant $c_2 > 0$. Consequently,

$$\mathbb{E}\{\Xi_n^2(\delta)\} \leq 2\mathbb{E}\{\tilde{\Xi}_n^2(\delta)\} + 2\mathbb{E}\{G_n^2(\delta)\} \leq 2(c_2 + 1)(n^{-1} + \alpha_n^2)\delta^2.$$

The proof for $W_2^2(\hat{\mu}, \mu) = O_P(n^{-1} + \alpha_n^2)$ is completed by setting $c_1 = 2(c_2 + 1)$. The result for

$W_2^2(\hat{\mu}, \tilde{\mu})$ follows from the same line of argument, conditional on Y_1, \dots, Y_n . \square

7 Function-valued Empirical Processes

In the proof of Theorem 3 we came across the problem of finding the convergence rate of a random quantity in the form $n^{-1/2} \sum_{i=1}^n h(\xi_i) \{\hat{g}(\xi_i) - g_0(\xi_i)\}$ for fixed functions h, g_0 and independent observations ξ_1, \dots, ξ_n such that $\mathbb{E}h(\xi_i)g(\xi_i) = 0$ for any g ; here \hat{g} is an estimate for g_0 based on ξ_1, \dots, ξ_n (and potentially on some other fixed quantities). For example, $\xi_i = A_i$, $h(\xi_i) = \pi(X_i) - A_i$, $g_0 = m_a$, and $\hat{g} = \tilde{m}_a$ in the proof of (S4), where we hold X_i fixed. Such a problem is also encountered in other scenarios of statistical research, for instance, in the proof of Theorem 9 of Mammen and van de Geer (1997). Unique in our context is that the function \hat{g} may take values in a space of functions, e.g., in the case of $\mathcal{W}_2(\mathcal{I})$, so that the classic results in van de Geer (1990) do not apply directly and need to be extended. Instead of function spaces, below we consider more generally a separable Hilbert space that includes some function spaces as special examples.

To set the stage, let \mathcal{X} be a compact space and ν a positive measure on it. Suppose that \mathcal{H} is a separable Hilbert space, and \mathcal{F} is a class of functions that maps \mathcal{X} into \mathcal{H} . An immediate example of \mathcal{H} is the space $L^2([0, 1])$ of real-valued squared integrable functions defined on $[0, 1]$. Consider an \mathcal{H} -valued random process S_n indexed by \mathcal{F} of the form

$$S_n(g) = \frac{1}{\sqrt{n}} \sum_{i=1}^n V_i(g),$$

where V_1, \dots, V_n are independent \mathcal{H} -valued centered random processes defined on \mathcal{F} . For instance, in the above context, $V_i(g) = h(\xi_i) \{g(\xi_i) - g_0(\xi_i)\}$ for each $g \in \mathcal{F}$.

Let η be a pseudo-distance on \mathcal{F} of the form $\eta^2(f, g) = n^{-1} \sum_{i=1}^n \eta_i^2(f, g)$, where η_1, \dots, η_n are also pseudo-distances on \mathcal{F} , e.g., $\eta_i(g_1, g_2) = \|g_1(\xi_i) - g_2(\xi_i)\|_{\mathcal{H}}$ with $\|\cdot\|_{\mathcal{H}}$ denoting the norm on the Hilbert space \mathcal{H} . Suppose $S_n(g_0) = 0$ for $g_0 \in \mathcal{F}$ and $\|V_i(g_1) - V_i(g_2)\|_{\mathcal{H}} \leq M_i \eta_i(g_1, g_2)$, where M_1, \dots, M_n are uniformly subgaussian random variables, i.e.,

$$\sup_i \mathbb{E} \exp\{\beta^2 M_i^2\} \leq \Gamma < \infty \quad (\text{S12})$$

for some absolute constants $\beta, \Gamma > 0$. Finally, let $\mathcal{K}(\delta, r)$ be the local entropy of a ball $B(r; g_0) \subset \mathcal{F}$ with respect to the pseudo-distance η . Without loss of generality we assume \mathcal{K} is continuous in δ ; otherwise, we just define it to be a continuous function that upper bounds the local entropy.

Theorem 5. *Suppose (S12) holds and $\mathcal{K}(\delta, r) \leq K\delta^{-2\zeta}$ for some $K > 0$ and $\zeta \in (0, 1)$. Then, there exist constants b_0 and c , depending only on β and Γ , such that for any $b \geq b_0$, we have*

$$\text{pr} \left(\sup_{g \in B(r; g_0)} \frac{\|S_n(g)\|_{\mathcal{H}}}{\{\eta(g, g_0)\}^{1-\zeta}} \geq b\sqrt{K} \right) \leq \exp \left(-\frac{cb^2K}{r^{2\zeta}} \right) \quad (\text{S13})$$

for all $n \geq 1$.

Proof. The subgaussian assumption implies that Eq (3.10) of Kuelbs (1978) is valid for $S_n(g_1 - g_2)$ for all $g_1, g_2 \in \mathcal{F}$. Then, (S13) follows from the argument that leads to Lemma 3.5 of van de Geer (1990). \square